
Aus dem Institut für Diagnostische Radiologie und Neuroradiologie
(Direktor Univ.- Prof. Dr. med. Norbert Hosten)
der Universitätsmedizin der Universität Greifswald

**Spacer-supported thermal ablation to prevent carbonisation and improve ablation
size: a proof of concept study.**

Inaugural – Dissertation

zur

Erlangung des akademischen

Grades

Doktor der Medizin

(Dr. med.)

der

Universitätsmedizin

der

Universität Greifswald

2023

vorgelegt von:

Fiona Mankertz

geboren am: 02.05.1996

in: Berlin

Dekan:	Prof. Dr. med. Karlhans Endlich
1. Gutachter:	Prof. Dr. med. Holger Lode
2. Gutachter:	Prof. Dr. med. Norbert Hosten
3. Gutachter:	Prof. Dr. med. Sönke Langner
Ort, Raum:	Universitätsmedizin Greifswald, Seminarraum P01.37
Tag der Disputation:	10.07.2023

Index	3
1 Introduction	4
2 Methods and Materials	10
2.1 Materials	10
Technical Material	10
Disposable Material	10
Digital Material.....	12
2.2 Methods	13
Laser ablation.....	13
Spacer	20
Experimental Setup	23
Methodical Analysis	27
Statistical Analysis	31
3 Results	33
3.1 Time Interval and Power Input	33
3.2 Reproduction Reliability	36
3.2 Interspatial Ablation Size	38
3.3 Intraspatial Ablation Size	41
4 Discussion	46
4.1 Spacer	49
4.2 Setting	52
4.3 Volumetry	54
4.4 Intraspatial Comparison	57
5 Conclusion and Outlook	60
6 Sources	62
7 Originalpublikation	74

Over the last decades the German Cancer Research Centre (DKFZ) has reported an increase in both incidence and prevalence of tumorous disease. In the span of 1990-2010, age-standardised incidence rose by 30% for men and 20% for women.

Simultaneously age-standardised prevalence increased by 80% for men and 35% for women. Among the main factors behind this increase, demographic changes, higher life expectancy as well as improved diagnostic modalities are named. [1]

It stands to reason that the increase in prevalence of tumorous disease has necessitated further development of therapeutic strategies. Besides conventional therapeutic options such as surgery, radiation therapy and chemotherapy (“Stahl, Strahl und Chemikal”), a greater focus has been placed on developing as well as studying the impact of minimally invasive techniques. [2] Due to pre-existing conditions, obscure tumour localisation as well as multiple preceding operations patients who do not qualify for general surgery are able benefit from minimally invasive procedures. [3] One of the most established and recognised techniques today is the concept of tumour ablation. [4]

Tumour ablation refers to the destruction of cancerous cells through an external stimulus. It is commonly divided into two subcategories: energy-based and non-energy based (**Figure 1**). Non-energy based ablation primarily focuses on chemical ablation through percutaneous ethanol and alcohol installation (PEI and PAI). Energy-based ablation can be divided into thermal-based and non-thermal-based modalities. Non-thermal tumour ablation consists of methods such as focused ultrasound and trans-arterial chemoembolization (TACE). Interstitial brachytherapy has also been developed over the past few years but is considered to be in its clinical infancy use and generally preferred for larger, auspiciously situated ablations. [5] The advantages of TACE have been sufficiently documented and are increasingly used in combination with thermal-based ablation. [6]

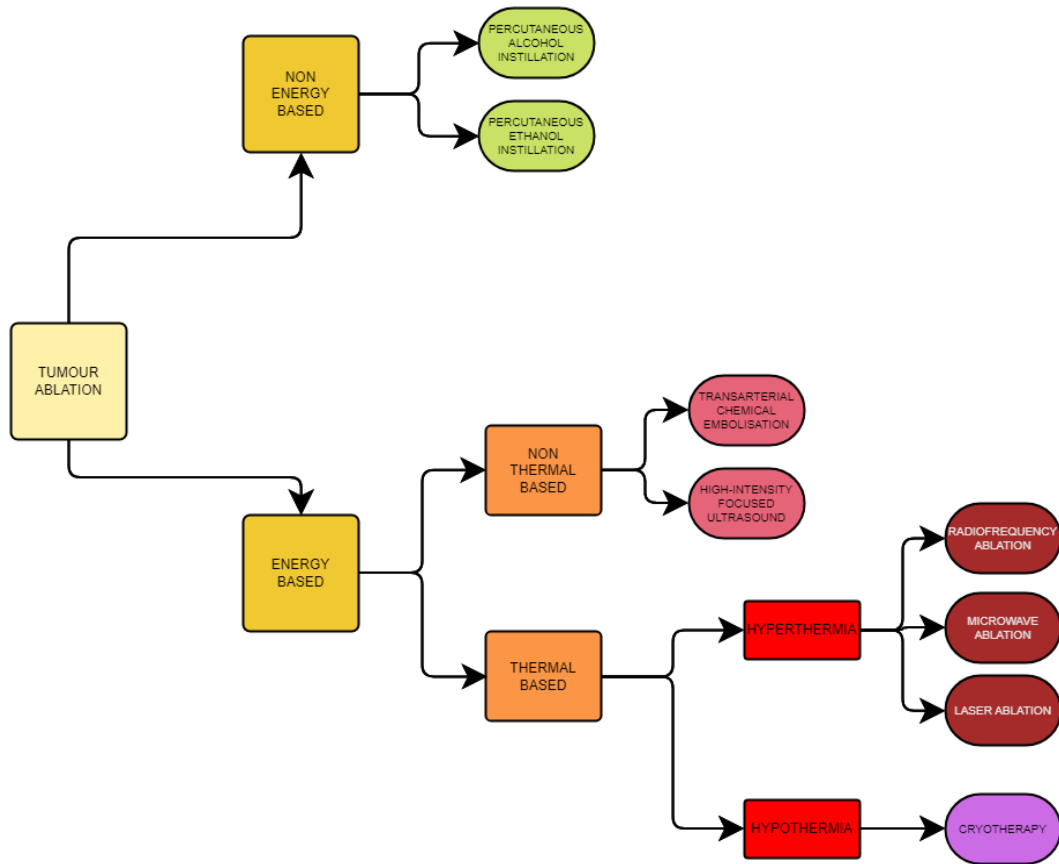


Figure 1: The main arms of tumour ablation.

At this point in time, thermal ablation comprises the majority of minimally invasive ablation. It utilises abrupt changes in temperature to fundamentally alter cell morphology and induce tissue ablation. Currently, the use of hypothermia in cryoablation is considered a model concept mostly used in renal cell cancer [7] and takes second place to hyperthermic ablation. Several competing methods of hyperthermic tumour ablations exist, the most common of which are radiofrequency ablation, microwave ablation and laser ablation. Radiofrequency ablation (RFA) creates energy and heat transmission through an alternating electric current. It is generally agreed upon as the most frequent method used in clinical practice. [8] A 2008 study reporting on 590 minimally invasive hepatic procedures noted that radiofrequency ablation was the second most common procedure with 240 separate interventions, only surpassed by minimally invasive resections (306 separate interventions). [9] It achieves good results and its long-term results are comparable to laparoscopic surgery, but it requires CT-guided imaging and cannot be used for

inauspiciously located tumours [10]. Microwave ablation (MWA) by means of electromagnetic waves has been considered a viable newer modality, however it is still in its infancy stage in regards to development and cost. [11] Laser ablation (LA) is less commonly used but agreed on as a cost-effective, scientifically established technique compatible with MRI imaging. [5, 12, 13]

The modalities of thermal ablation may differ in their physical properties and respective indications, however they all share the same aim: the complete thermal ablation of tumorous tissue with an adequate margin of non-tumorous tissue. Its biggest limitation in doing so has proven to be maximum achievable ablation size. [14]

Ablation size (both in volume and diameter) is limited due to the periprocedural transformation of vital energy-conducting tissue into a boundary layer which does not conduct energy efficiently. In thermal ablation this process is known as carbonisation. Carbonisation occurs when tissue temperatures rise above 100°C. As biological tissue is sensitive to external stress, a sudden increase in temperature leads to protein denaturation, the dissolution of hydrogen bonds and DNA polymerase inhibition. [15] At temperatures of over 45°C, irreversible cell damage occurs. This process is sped up exponentially with further increase in temperature; it is the principle on which thermal ablation of tumorous tissues relies on. However, when tissue temperatures exceed 100°C, the affected tissue is charred and desiccated as gaseous microbubbles form and vaporisation occurs. [16] Carbonisation naturally develops primarily in zones with the highest tissue temperature. This translates to the central zone around the applicator in LA [17], around the needle electrodes in RFA [18] and around the antennae in MWA. [19] The carbonised area around the ablation probe acts as an insulating border: a boundary layer. It hinders the effective diffusion of energy into peripheral tissue due to its physiological properties. This insulation consequently limits ablation size. [20, 21] Additionally, in laser ablation photons are backscattered from the surrounding tissue onto the carbonised area. This further increases the temperature around the ablation probe. [22] As a result, damage to the laser fibre occurs.

Several innovations have been developed to delay or prevent carbonisation, such as the introduction of an internal cooling system for both radiofrequency ablation and LA. This concept relies on a continuous diffusion of cooling fluid directly surrounding the probe, which lowers the central temperature and delays the formation of carbonisation for a limited time. [23] A miniaturised laser applicator with an integrated thermoregulation system was developed by Hosten et al. in 2003, which increased ablation size. [24] A more complicated, but effective strategy is the reduction of arterial blood flow and thus the elimination of the heat sink effect. These strategies include total portal flow occlusion through Pringle manoeuvre, angiographic balloon occlusion as well as intraarterial embolization. [20] The Pringle manoeuvre as well as other vascular clamping techniques have shown a greater efficacy in ablation size when additionally conducted. However, they harbour the risk of ischemia-reperfusion syndrome especially in patients with hepatic steatosis or fibrosis of the liver. [25, 26] The use of intermittent versus continuous clamping has been debated, both of which have its advantages and disadvantages when it comes to ischemia time and risk of intraoperative haemorrhage. [27]

However, even with continuous scientific improvements made to increase ablation size, limitations to its efficacy remain. The development of an internally cooled laser applicator by Vogl et al. allowed the ablation of up to 33 mm diameter. [28] According to Regier et al., “more than 95% of [hepatic] tumours under 30 mm in diameter can be completely ablated”. [29] A review study conducted by Stroszczyński et al. in 2004 reported that even with multiple applicators tumours ≥ 50 mm couldn't be ablated due to the lack of a proper safety margin. [30] Ahmed et al. reported that tumours < 30 mm could be fully ablated in 100% of all cases, whereas that was only the case for 38% of all lesions between 30-50 mm. [31]

In contrast, most hepatic tumours are more than 30 mm in diameter. [32] Two studies conducted by the Barcelona Clinic Liver Cancer (Hospital Clínic de Barcelona) and the Hepatico-Pancreatico-Biliary Surgery Unit (The Royal London Hospital) found that mode and median tumour size were both 50 mm. [33, 34] 84% of metastases were reported as 50 mm in surgery, as well as 78% in chemotherapy. A 2018 study by

Wu et al. reviewing 57920 patients with hepatocellular carcinoma found a median tumour diameter of 59.7 mm. [35] A 2020 study reported a mean diameter of 42 mm when reviewing 58 HCC cases. [36] The BCLC does not recommend thermal ablation as a viable method for hepatic tumours > 30 mm in diameter and explicitly recommends choosing surgical resection for tumours > 50 mm. [37]

The above studies offer little answers on how to treat tumours falling into the “intermediate” category between 30-50 mm. Weigel et al. do not recommend the ablation of any lesion larger than 30mm. [38] Covering a wider coagulative volume and diameter has up until today only been accomplished through the use of 2+ applicators. According to Vogl et al. the greatest mean volume that has been achieved with a single applicator in five repeated experiments is 22.4 cm³ (an increase by a 5.3 factor of change in comparison to earlier results of 4.2 cm³). [28] Additionally, with every additional applicator placed the risk of perforation as well as necrotic inhomogeneity and discomfort to the patient increases. Pruitt et al. reported an increase of postinterventional complications when using multiple applicators and recommended limiting the use when possible. [39] An alternative method to multiple applicators would not only mean further development of an already established treatment, but would also come with significant risk reduction.

We can conclude that at the current point in time it is not possible to ablate most hepatic tumours in toto. There is, in summary, a gap between *achievable* and *desirable* ablation size.

An approach to bridging this gap is the use of a spacer to prevent carbonisation and increase ablation size. Implementation of a spacer in ablation therapy was expanded on in a different setting: the use of a spacer during focal prostate ablation has been proven to prevent heat damage to surrounding organs. In a 2021 study Namakshenas et al. report that rectal temperatures were significantly lower when a polyethylene glycol spacer surrounding the laser applicator was utilised. [40] Ishikawa et al. found in a 2023 study that the inclusion of a hydrogel spacer before hypofractionated irradiation reduced number of fractions needed and increased fraction size, resulting in more effective treatment. [41] Björelund et al. additionally noted that

the implantation of a hyaluronic acid spacer in radiotherapy of prostate cancer significantly reduced genitourinary and gastrointestinal late-stage toxicity. [42]

We developed a spacer prototype for laser ablation by means of cooperation between the AG “Experimentelle Radiologie” (Universitätsklinikum Charité, Berlin) in cooperation with the Institut für Diagnostische Radiologie und Neuroradiologie (Universitätsmedizin Greifswald, Greifswald). Our hypothesis was that a spacer would extend the distance between initial photon emission from the optical fibre and photon ingress into the targeted tissue and additionally, by building on the principle of the cooling system, reduce central tissue temperatures, prevent carbonisation and subsequently increase ablation size. We studied the impact of a spacer’s presence for laser ablation in an ex vivo liver model. The study’s findings were accepted for publication on February 13th 2023 and published under the title “Spacer-Supported Thermal Ablation to Prevent Carbonisation and Improve Ablation Size: A Proof of Concept Study” in *Biomedicines*. [43]

This study aims to ascertain whether the use of a spacer-supported laser applicator system results in an increase in ablation size. We created two spacer prototypes and measured both ablation volume as well as the smallest ablation diameter. These results were then compared to those of a stand-alone applicator system and the presence of statistical significance was investigated. Any differences between the spacer-supported applicator system and standalone applicator system will be referred to as **interspacial**. Any differences between the two spacer prototypes will be referred to as **intraspacial**.

2 METHODS AND MATERIALS

2.1 MATERIALS

TECHNICAL MATERIAL

Medilas fibertom 5100 Laser	Dornier MedTech, Munich, Germany
Medilas fibertom 5100 Optical Fibre Connector with sheath	Dornier MedTech, Munich, Germany
Medilas fibertom 5100 Laser Protection Goggles	Dornier MedTech, Munich, Germany
Perfusor segura FT	B. Braun Parchim AG, Melsungen, Germany
Original-Perfusor® Syringe 50 ml	B. Braun Melsungen AG, Melsungen, Germany
R95E Infrared lamp 230 V, 100 W	Philips, Koninklijke Philips N.V., Amsterdam, Netherlands
ClinScan 70/30 USR MRI	Bruker Biospin GmbH, Bruker Scientific Instruments, Ettlingen, Germany
Bio R.Bed 72 MRI Slider	Bruker Biospin GmbH, Bruker Scientific Instruments, Ettlingen, Germany
90430 Steel Thermal Isolation Box 350 ml	Reer GmbH, Leonberg, Germany
KWMOBILE Digital Thermometer	KW-Commerce GmbH, Berlin, Germany
E-4038 Measuring Cylinder 500 ml	neoLab Migge GmbH, Heidelberg, Germany

DISPOSABLE MATERIAL

Optical fibre	RoweCath, RoweMed AG - Medical 4 Life, Parchim, Germany
Sterile Surgical Tape	RoweCath, RoweMed AG - Medical 4 Life, Parchim, Germany
Perfusor tubing PE 800 mm	RoweCath, RoweMed AG - Medical 4 Life, Parchim, Germany

5,5F PTFE catheter	RoweCath, RoweMed AG - Medical 4 Life, Parchim, Germany
5,5F PTFE catheter lock	RoweCath, RoweMed AG - Medical 4 Life, Parchim, Germany
4,5F titanium trocar	RoweCath, RoweMed AG - Medical 4 Life, Parchim, Germany
Y-Piece with haemostatic valve	RoweCath, RoweMed AG - Medical 4 Life, Parchim, Germany
Liver	LandWert Hof, Stahlbrode, Germany
20 ml Mini-Plasco Aqua ad iniectabilia Injection Solution	B. Braun Melsungen AG, Melsungen, Germany
20 ml Mini-Plasco NaCl 0,9% Injection Solution	B. Braun Melsungen AG, Melsungen, Germany
5 ml Injekt Luer Solo Syringe	B. Braun Melsungen AG, Melsungen, Germany
Combi Stopper Closing Cone	B. Braun Melsungen AG, Melsungen, Germany
Feather Disposable Scalpel #10	Andwin Corporation, Woodland Hills, CA, United States
Durapore Surgical Tape 2,5 cm x 9,1 m	3M Company, Maplewood, MN, United States
Peha-soft nitrile gloves S 6-7	Paul Hartmann AG, Heidenheim an der Brenz, Germany
Mikrozid® Universal Wipes Premium	Schülke & Mayr GmbH, Norderstedt, Germany
Saran Wrap 29 cm x 75 m	Home Ideas Cooking, Rel Group, Cologne, Germany
Felt-tip Pen Fine/Reg	Viscot Medical LLC, East Hanover, NJ, United States
Laminated Cards	In-house production

DIGITAL MATERIAL

Horos DICOM Viewer	Purview, Nimble Co LLC, Annapolis, MD, United States
<i>syngo</i> ®.MR General Engine B15	Siemens Healthcare GmbH, Erlangen, Germany
Microsoft® Word LTSC MSO (16.0.14332.20458) 64-Bit	Microsoft Corporation, Redmond, WA, United States
Google Sheets Spreadsheet Program	Google LLC, Mountain View, CA, United States
IBM SPSS Statistics	IBM Corporation, Armonk, NY, United States

2.2 METHODS

LASER ABLATION

The acronym “laser” stands for “**L**ight **A**mplification by **S**timulated **E**mission of **R**adiation” and was coined by Gordon Gould in 1959. It is used when referring to both a lasing medium and its mechanism of excitation through a suitable power source. This power source can be electrical, chemical or optical. The laser used in this study was a neodymium-doped yttrium aluminium garnet (Nd:YAG) with a wavelength of 1064nm. A laser can be classified through their mode of operation: continuous wave or short pulse wave. [44] Lasers in thermal ablation commonly utilise continuous wave. As such, all following discussion will be made with the principle of continuous wave emission as a precept. [45] Electrons in a lasing medium such as glass, liquid, gas or certain crystals absorb energy from light (photons) or heat (phonons). These electrons then transfer to a higher energy state in the nuclear orbit. When the electrons transition back to a lower energy state, the additional energy is released through photons in a process called *stimulated emission*. The emitted energy is able to interact with the target tissue in several ways. It can be transmitted through tissue, reflected or refracted back, scattered or absorbed. Opaque biological tissue, such as the one of organs, is inherently turgid and prevents significant transmission or reflection. [46] For example, the biological quality of hepatic tissue is marked by a high melanin and haemoglobin chromophore content. Nd:YAG lasers show a high absorption coefficient when they are used in tissue with a high content of melanin and haemoglobin. [47] In this tissue, their laser-tissue interaction consists mainly of absorption and scattering. As such, Nd:YAG lasers are uniquely suited to ablation of hepatic tissue. [48]

Name of laser-tissue interaction type	Mechanism
Photothermal	Heat transfer to surrounding tissue via absorption and exchange of kinetic energy provided by the laser
Photochemical /Photodynamic	Chemical reaction caused by the absorption of laser energy by photosensitive molecules
Photoablative	Non-thermal breaking of chemical bonds through energetic photons
Photoplasmic	Strong photoionization of the tissue followed by energy absorption from spontaneously formatted plasma
Photodisruptive	Mechanical tissue rupture caused by plasma formation and acoustic shockwaves.

Table 1: Types of thermal damage.

During the lasing process several laser-tissue interactions take place, the biggest factor in which is photothermal interaction (**Table 1**). [49–51] When the laser beam passes through the target tissue, photoexcitation takes place as the tissue absorbs the laser beam’s photons and therefore its energy. The absorbed energy is diffused throughout the environment, and leads to thermal conduction: heat is generated and transmitted into the cellular environment where it causes focal hyperthermic injury. This bioheat-transfer process causes the surrounding tissue to be damaged. [52] Cell damage is dependent on tissue temperature and exposure time: at temperatures of > 45°C cells are irreversibly damaged. Tissue coagulates and irreversible protein denaturation occurs, leading to DNA polymerase inhibition and cell membrane dissolution. This process is exponentially shortened when tissue temperature is further increased to > 60°C, a point in which collagens are denatured. This threshold of 60°C is therefore considered vital for almost instantaneous ablation of malign cells and surrounding tissue. [28, 30, 53]

When tissue temperature reaches 100°C the targeted tissue's cell structure transforms further. This process is described as "carbonisation". [54] Carbonisation is the pyrolysis of organic tissue into a carbonaceous material. In the lasing process, carbonised tissue absorbs the light emission to a higher degree than the surrounding non-carbonised tissue. Due to the tissue's carbonaceous state and high light absorption, this prevents heat propagation into the surrounding tissue. [55] Ablation size is limited as tissue further from the optical fibre cannot attain a state of photoexcitation and photothermal cell damage. In addition, due to vaporisation other energy-tissue processes such as reflection and refraction take place in carbonised tissue. [56] The laser photons are reflected onto the optical fibre itself. This causes damage to the diffuser and fibre and the lasing process is prematurely aborted. [57] Therefore, the ideal temperature for laser ablation must be maintained between 60°C and 100°C to avoid carbonisation. [58] Stafford et al. as well as Patel et al. additionally recommend a 10°C safety buffer to prevent heat spikes and possible damage done to the fibre and catheter. [53, 59] In line with those findings this study's aim was to keep temperatures between **60°C and 90°C**. [31, 53, 60]

Laser ablation is only as effective as the tissue it is applied to. Due to the high vascularisation of hepatic tissue, tissue temperature may be lowered by the cooling blood flow perfusion of nearby vessels. This "heat sink effect" is responsible for the reduction of overall ablation size and may prevent complete tumour eradication. [61] The heat sink effect is particularly relevant to in vivo studies due to the diminished ablation size near large blood vessels. [31] Additionally, pre-existing conditions like hepatic steatosis or cirrhosis are likely to cause inaccuracy when predicting ablation size and volume. These variables serve to increase pre-existing heterogeneity of heat deposition: closest to the laser applicator the heat distribution will be highest, while further from the applicator it lowers exponentially. [62] Despite the difficulty of predicting in vivo ablation sizes, a study by Fahrenholtz et al. found that there was acceptable overlap between predicted and measured ablation size and volume. [63]

In this study a Medilas fibertom 5100 was used. The Medilas fibertom 5100 and all relevant lasers used in ablation therapy are classified as Class IV lasers by DIN EN

60825-1 Ordinance. Exposed laser light is classified as very dangerous for optical and dermal tissue. [64] Scattered light is able to cause severe injury when viewed without protective eyewear. The handling of Class IV lasers requires proper safety training and an adequate environment. [53] In this study, any and all ablation procedures were conducted in a locked room with the appropriate signage discernible to external viewers or personnel. This included hazard signs to signify the class and power of the laser used and possible remote damage. Additionally, the laser was outfitted with a primary key switch and a secondary manual foot switch to ensure prompt cessation of radiation if needed.

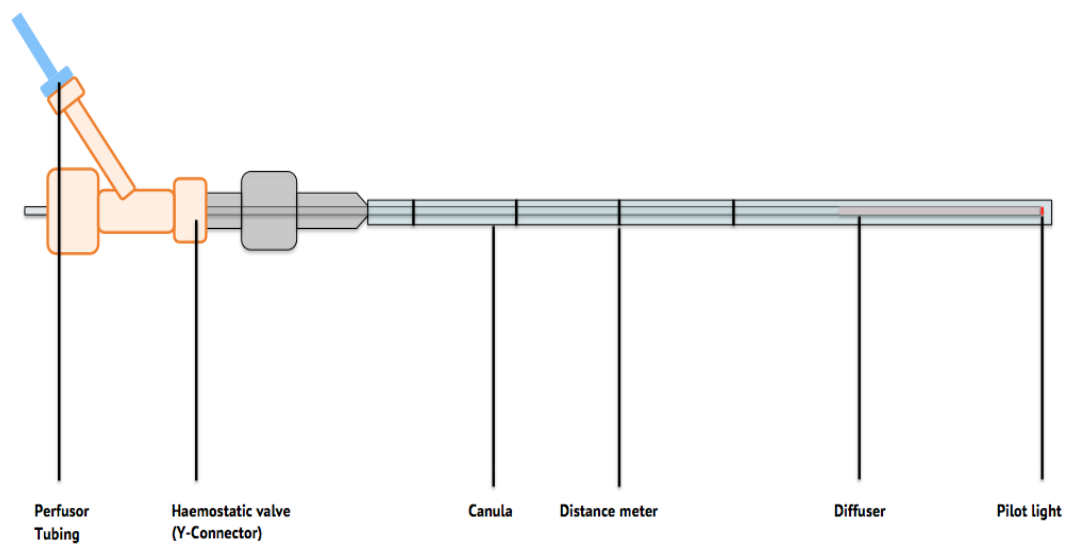


Figure 2: Laser applicator.

The stand-alone applicator system without a spacer was developed through RoweMed (RoweCath, RoweMed AG, Parchim, Germany) for clinical use (**Figure 2**). It consisted of a miniaturised applicator system with an internal cooling mechanism. The system can be divided into three separate subsets which will be highlighted separately.

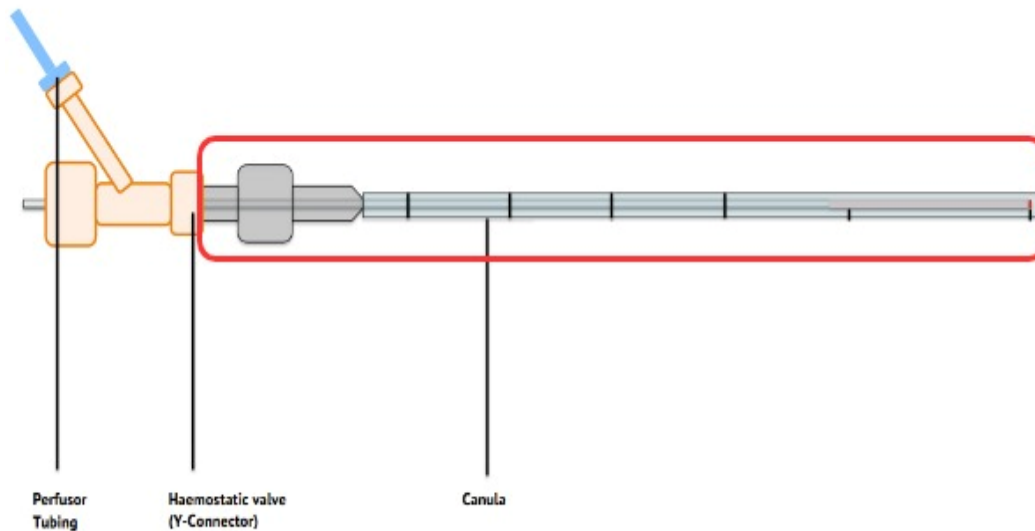


Figure 3: Optical fibre and scattering body.

1. A 4,5 F (1,5 mm) titanium trocar and its enclosing transparent 5,5 F (1,8 mm) PTFE diffusion catheter with 10 mm depth gauges (**Figure 3**). The tetragonally-tipped trocar was used to perforate the liver capsule and ease the way for the heat-resistant PTFE catheter. It was then removed and replaced by the optical fibre. The catheter additionally had a lancing depth limit and a female luer lock adapter. Its width was specifically developed to allow minimal fluid flow between the optical fibre and the catheter's inner wall in order to cool the diffuser tip. [55]

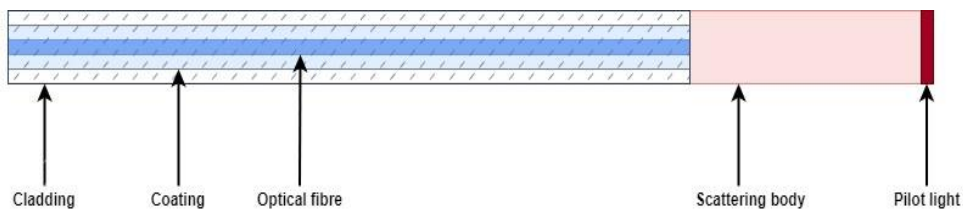


Figure 4: Optical lasing fibre and scattering body.

2. The phrase "optical fibre" will subsequently be used as an umbrella term to refer to the fibre's components: an optical fibre connector, the optical fibre itself and a connected scattering body (Dornier Diffusor Tip H6111-T3; Dornier, Wessling, Germany). The optical fibre connector spliced the fibre with the laser (Medilas fibertom 5100; Dornier, Wessling, Germany) and transitioned into the optical fibre's doped quartz glass core. The quartz core was encased by a quartz glass sheath ("Cladding") and again by a synthetic outer jacket ("Coating") (**Figure 4**). The Cladding sheath had a significantly lower refractive index than the quartz core. Due to this lower refractive index any emitted light was continuously reflected back to the core: an optical phenomenon called total internal reflection. [65] The synthetic Coating jacket prevented the emission of light in case of cable rupture or defective manufacturing. It had a slightly higher refractive index than the quartz Cladding, so any erroneous light was absorbed. The combination of Cladding and Coating allowed the light to travel through the fibre without significant loss of energy. [66] Close to the optical diffuser tip the Coating and Cladding tapered into a non-coated flexible fibre. This fibre connected to the scattering body through which radial light was emitted into the surrounding tissue. This scattering body was outfitted with a pilot light which emitted a homogenous red light as an indicator of the laser's correct functionality. The diffuser tip acted as the focal point through which energy was transferred into the tissue.

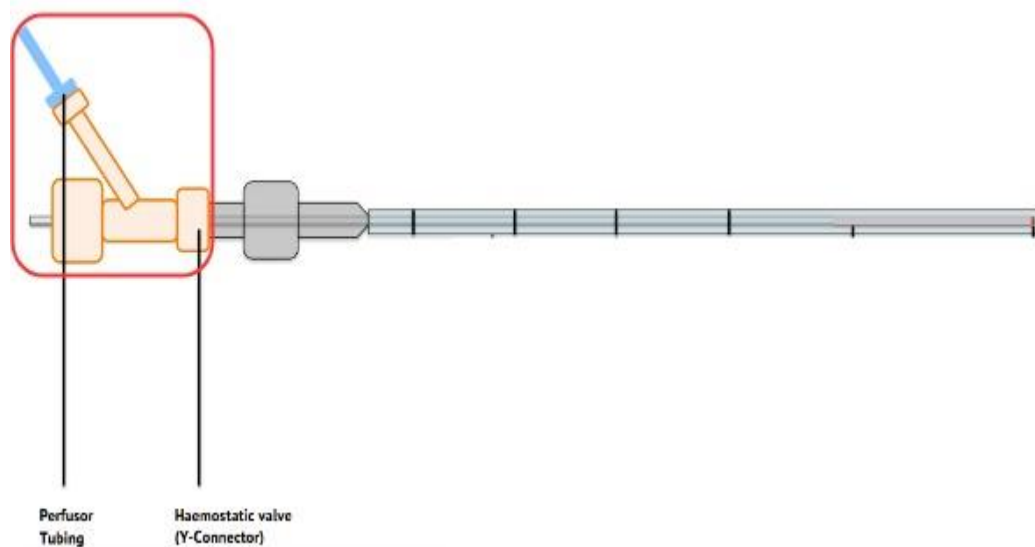


Figure 5: Y-Connector and perfusion tubing.

3. A Y-Connector with a male luer lock main port connecting to the PTFE catheter and a female luer lock side port connecting the perfusor tubing (**Figure 5**). Its outside lumen was locked through a haemostatic valve. This positioned the optical fibre axially and prevented reflux of blood or cooling fluid when used in vivo. The perfusor tubing transmitted the cooling fluid over a standardised length of 800 mm and connected distally to a 50 ml hypodermic syringe attached to a standard dual-processor perfusor. Its perfusion flow rate ranged from 0,01-99,9 ml/h but was set to 60 ml/h for the duration of this study. The flow rate is further discussed in **4 Discussion**.

Both spacer types were developed and custom-built by hand by Prof. Dr. rer. nat. U.S. and Dr. med. vet. O.G. (AG “Experimentelle Radiologie” Charité, Berlin, Germany). Its structure can be differentiated into three components: a corpus, a tip and a Y-Piece. When referring to “spacer” we refer to those three components.

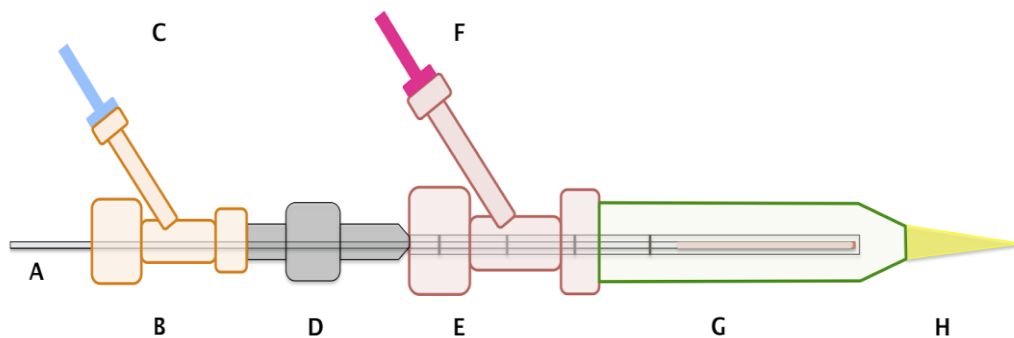


Figure 6: Closed spacer-supported applicator system.

A: Optical fibre. B: Applicator Y-Piece. C: Perfusor tubing. D: PTFE catheter. E: Spacer Y-Piece. F: Drain tubing. G: Glass corpus. H: Pipette tip.

The closed spacer’s blueprint is depicted in **Figure 6**. The closed spacer’s main body (**G**) consisted of a cylindrical glass corpus (\varnothing 4 mm) similar in form to a centrifugal tube. Distally it connected to a 200 μ l polypropylene pipette tip (**H**). This tip’s distal orifice was also manually closed off through UV glue. The comparatively sharp tip of the pipette allowed for easy insertion into the liver tissue, similarly to the standard applicator’s trocar. The main body’s proximal opening connected to a Y-piece (**E**) with a female luer lock side port and a male luer lock main port. During the ablation process drain tubing (**F**) was attached to the side port, which drained heated fluid to an insulated calorimeter. Inside the calorimeter the average temperature of the drained fluid was measured. The main port connected to the pre-existing applicator system’s

own PTFE catheter (**D**) which was itself attached to its own Y-Piece (**B**) at its proximal end. The applicator Y-Piece had a female luer lock side port through which perfusor fluid was diffused into the spacer (**C**).

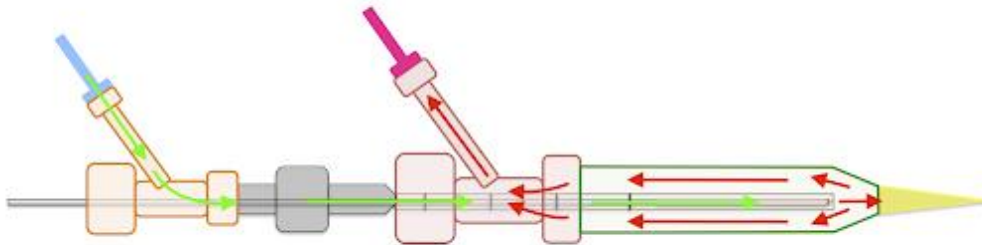


Figure 7: Fluid diffusion within the closed spacer.

Green arrows: Fluid influx. Fluid travels through Applicator Y-Piece and PTFE catheter distally until it emerges from the distal end of the diffuser. Red arrows: Fluid efflux. Fluid travels through the spacer tip and main body distally until it is drained into the side port of the spacer Y-Piece and into the drain tubing.

Figure 7 shows the flow of cooling fluid through the spacer. Fluid was diffused through the PTFE catheter and distally entered the glass spacer. It then flowed backwards into the drain tubing.

3.1.3 Spacer-supported open applicator system

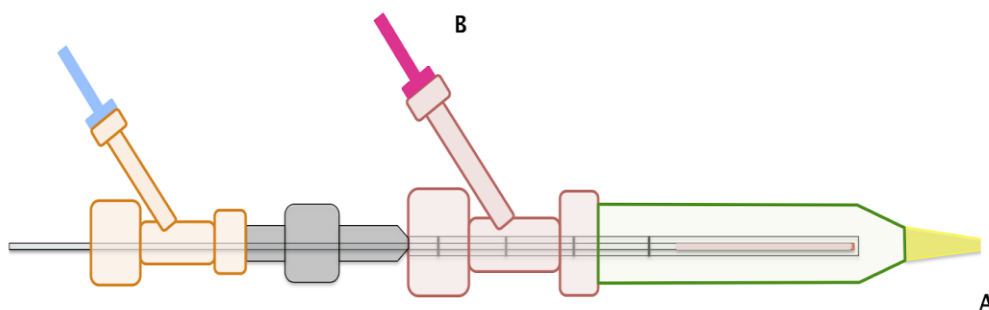


Figure 8: Open spacer-supported applicator system.

The open spacer in **Figure 8** featured a similar structure to the closed spacer with the exception of the 200 μl pipette tip (**A**). This pipette tip remained open-ended with a tip diameter \varnothing 0.6 mm. Drain tubing was attached, but we found no significant amount of fluid drained through it. Therefore, the diffusion of fluid in **Figure 9** was redirected towards the distal orifice.

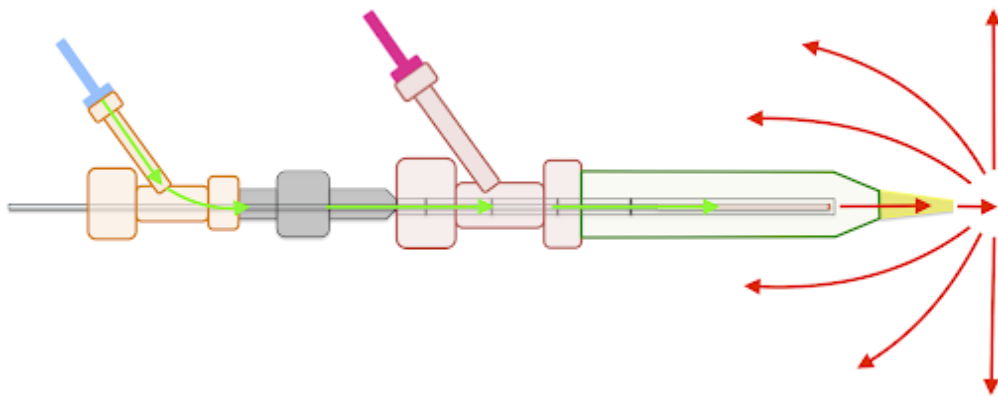


Figure 9: Fluid diffusion within the open spacer.

To ensure realistic ex vivo simulation bovine livers were chosen over porcine livers. This was due to bovine hepatic tissue possessing macroscopic and histological similarities to human hepatic tissue. For example, both have a similar hepatic capsule density. [67] The livers were acquired from an organic abattoir (LandWert Hof, Stahlbrode, Germany) <1h post-slaughter and transported in a heat-resistant Styrofoam container for lab samples. Pre-transport they were expressly kept warm through the means of infrared lighting and a body-warm bath. During the transport temperature was measured and adjusted to keep a steady 37°C (98,6 °F) in order to keep near-normothermic conditions as advised by Viard et al. [68] All livers (n = 15) were delivered in this manner. Pre-ablation they were examined by a public health veterinarian and deemed to show no pathological characteristics or otherwise be unfit for medical-grade experimentation. Any remains of adjunctive structures and omental fat were removed to ensure tissue homogeneity. Large vessels like the hepatic portal vein, caval veins, hepatic arteries, or the biliary duct were longitudinally incised. This was done to prevent diffusion into them. Furthermore, the caudate lobe and any parts of the liver deemed too shallow for applicator perforation were removed. The hepatic tissue was prepared to have a safety margin consisting of a 100 mm radius on each side. This was done to simulate proper heat transfer in a fully developed organ and avoid the abortion of the ablation process due to lack of space. [56]

The insertion process of the fibre applicator into the liver tissue was largely identical when utilising the stand-alone applicator system (S_N), the spacer-supported applicator system with an open-ended spacer (S_O), and the spacer-supported applicator system with a close-ended spacer (S_C). Relevant differing measures will be pointed out subsequently.

After bedding the pre-cleaned liver onto an even surface its capsule was incised with a scalpel (S_C , S_O) or trocar (S_N) to ensure a smooth transition into the liver tissue (**Figure 10a**).

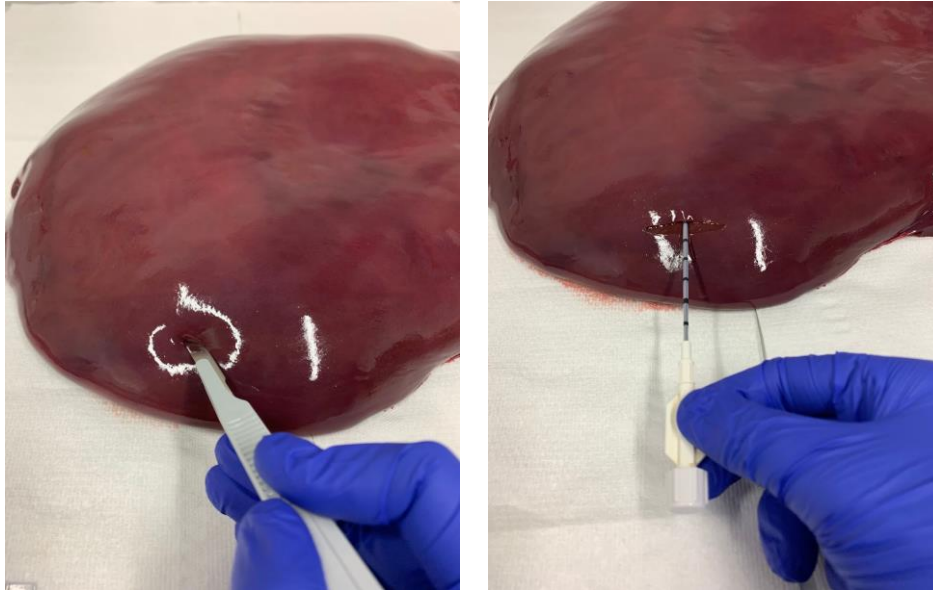


Figure 10. a) Tissue preparation through incision of the hepatic capsule. b) Insertion of the trocar and PTFE catheter.

INSERTION OF THE STAND-ALONE APPLICATOR SYSTEM:

After puncture the trocar was removed and combined with its matching PTFE catheter. This combination was inserted into the tissue, making sure that a minimum insertion depth of 100 mm was reached to assure full development of the ablation with enough surrounding unharmed tissue (**Figure 10b**). After sufficient insertion depth had been reached, the catheter's depth was marked and both catheter and trocar were retracted. The trocar was temporarily put aside while the distal part of the catheter was connected to the main port of the system's Y-Piece.

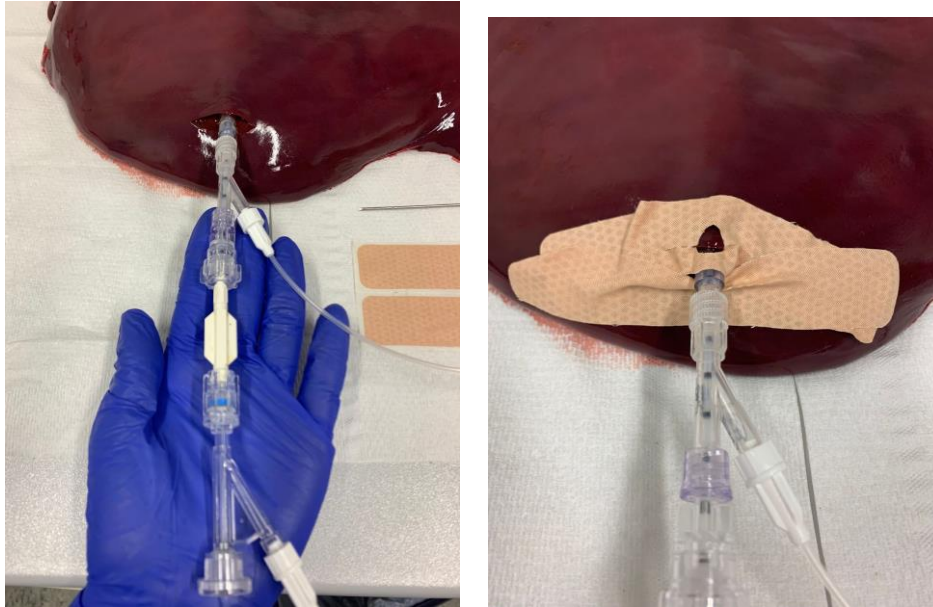


Figure 11. a) Insertion of the applicator system. b) Fixation of the spacer body with surgical tape.

The optical fibre was inserted through Y-Piece and catheter (**Figure 11a**), capping off <1 mm from the catheter's distal opening. This line-up was crucial to ensure satisfactory lavation of both diffuser and pilot light, therefore minimising the risk of overheating and damage to the optic fibre. The haemostatic valve was tightened to prevent involuntary movement of the fibre; afterwards the perfusor was connected with the female luer lock side port via perfusor tubing. The perfusor was set to 60 ml/h and enough time was given to ensure the complete filling of both perfusor tubing and PTFE catheter. The laser itself was switched on ca. 10 seconds after complete filling of the PTFE catheter was manually observed. Both PTFE catheter and its enclosed optical fibre were inserted up to the marked point and stabilised with 30 mm of surgical tape. If the applicator system was deemed to tilt or appear crooked, it was further stabilised with surgical tape (**Figure 11b**), height equalisers such as a narrow box or if deemed inoperable, retracted and inserted again.

INSERTION OF THE SPACER-SUPPORTED APPLICATOR SYSTEM:

The spacer itself was first connected to a fitting PTFE catheter. Due to the spacer's prolonged length 180 mm catheters were required, which were inserted until the tip lined up with the shank of the glass corpus. At the proximal end of the catheter the main port of the pre-existing Y-Piece was attached and locked. Before attaching

the proximal and distal tubing for perfusor and calorimeter the spacer first had to be filled with water. To prevent leakage a closing cone was attached to the distal side port (S_o) and the proximal haemostatic valve was tightly locked. The proximal side port was used to fill the spacer with 0.9% sodium chloride until fluid was beading out of its distal orifice (S_o) or distal side port (S_c). After the syringe was completely filled it was detached and the perfusor line was attached to the proximal side port. The perfusor line had been previously filled with fluid to avoid air being pushed into the fluid-filled spacer and potentially disrupting the water flow. The optical fibre was then inserted through the haemostatic valve and passed through the proximal Y-Piece, catheter and spacer until its diffuser tip capped off <1 mm from the inner catheter's distal opening.

After that, both haemostatic valves - the distal one belonging to the spacer system and the proximal one belonging to the pre-existing applicator system - were tightened and the spacer was inserted through the incision in the liver capsule. Its insertion compared to S_N in that a minimum insertion depth of 100 mm was marked on the spacer. Post-insertion the spacer was either flushed to ensure any clogging of the distal orifice was eradicated (S_o); or its distal side port was connected to the calorimeter via drain tubing (S_c).

To start the ablation process, the laser itself was manually turned on and the optical fibre connected via fibre connector. The desired power input was chosen and the safety lock disabled before starting the laser through use of a foot-operated floor switch. Any overheating with subsequent carbonisation and charring of not only the immediate tissue but also the diffuser and optic fibre was forewarned by activation of the Lightguide Protection System (LPS). [59, 81-83] The ablation procedure consisted of activating the laser manually once the applicator system was inserted inside the hepatic tissue. There were two outcomes: either the desired timeframe passed without activation of the LPS, or the LPS activated and the trial was cut short.

We conducted two main trials: an *interspatial* comparison between the two spacer-supported applicator systems and the stand-alone applicator, as well as an *intraspatial* comparison between the closed spacer prototype and the open spacer prototype.

MRI VOLUMETRY

All MRI scans were done through a 7T ClinScan 70/30 Biospec MRI USR (Bruker Biospin GmbH, Bruker Scientific Instruments, Ettlingen, Germany) MRI was chosen because of its propensity for clear soft-tissue imaging and ability to commit to thermometry in real-time periprocedural imaging. This allows quick feedback and action to be undertaken if necessary as well as allows the possibility of monitoring the extent post-procedural ablation through perivascular heat diffusion. [69, 70] MRI-supported procedures also show a higher postinterventional lesion-focused ablation rate than sonography-supported procedures. [71] Goldberg et al. describe MRI-guided imaging as the “only modality with well-validated techniques for near real-time temperature monitoring”. [72] Its lack of radiation exposure makes it uniquely suitable for children or palliative patients. The exception to that are patients with older pacemakers or other implanted cardiac devices, but the stand-alone applicator system as well as the spacer possesses no metal components and is therefore suited to MRI usage. [30, 31] Despite the experiments being conducted wholly ex vivo, this specific MRI was chosen due to its suitability for animal studies. Previously, the same MRI had been utilised for establishment of an animal model for research on arterial hypertension and myocardial hypertrophy with *cyp1a1ren-2* transgenic rats. [73]

T1 weighted FL2D imaging was chosen due to the compromise between high quality and clear tissue/ablation borders and relatively low imaging time. Several preliminary test runs were attempted (n = 11) to showcase any differences between long imaging (45 min) and short imaging (15 min), but none showed any significant difference in image quality when reviewed by the author, the MRI’s medical-technical assistant Mr S.H. and research associate Dr. med. vet. S.M.

To prepare relevant ablation areas for imaging, pieces of the liver were individually excised post-procedurally and secured in saran wrap (**Figure 12a**). The first excision was done with a proper border of vital tissue to allow comparison between vital tissue and ablation in the MRI. These tissue blocks were then placed on the MRI slider and inducted into the MRI corpus (**Figure 12b**).

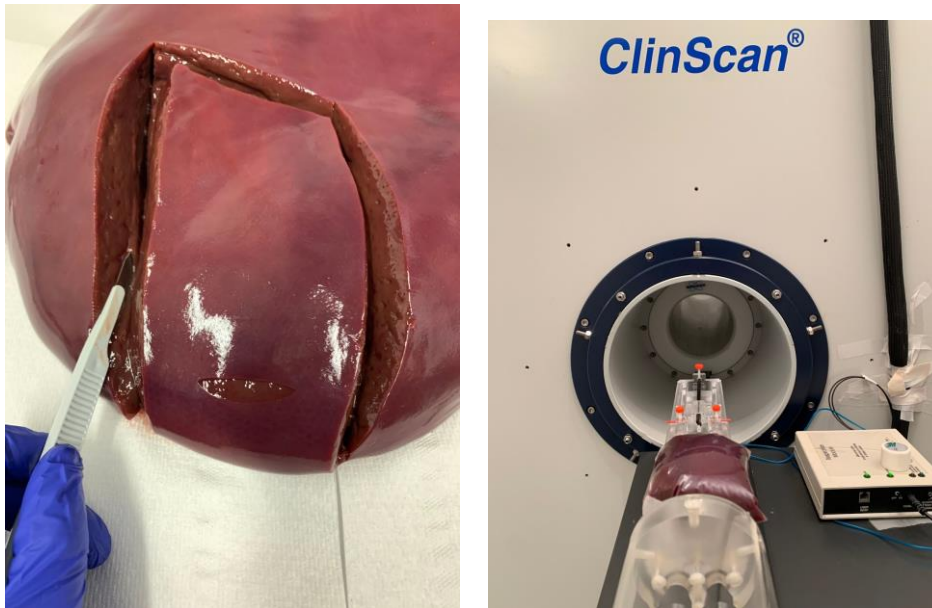


Figure 12. a) Initial liver excision before volumetry. b) Induction of the excised liver into the MRI.

The liver pieces were examined and volumetried through the DICOM software viewer Horos. Standard procedure was here to select the two sequences running through the sagittal and horizontal plane and calculate the area through a closed-polygon border estimation. These areas were measured in every image of the sequence, excluding those where ablation was non-existent. Following a conclusive area selection, the ablation' volume was calculated through ROI volumetry and photographed from all sides to ensure proper documentation. This is further discussed in **4.3 Volumetry Discussion**.

DISPLACEMENT VOLUMETRY

Ablation volume was additionally manually measured through displacement volumetry. It was then compared to the ablation calculated by ROI volumetry to prevent type I errors and false positive results. Displacement volumetry relies on Archimedes' principle that the force buoying a submerged object is equal to the weight of the fluid displaced by the object (**Figure 13**).

$$F = \rho Vg \leftrightarrow m = V \rho$$

$$\therefore V = m$$

F = Object buoying force [N]

ρ = density of the displaced fluid [kg/m³]

g = gravity of Earth [N/kg]

m = mass of the displaced fluid [g]

V = volume of the buoyant object [cm³]

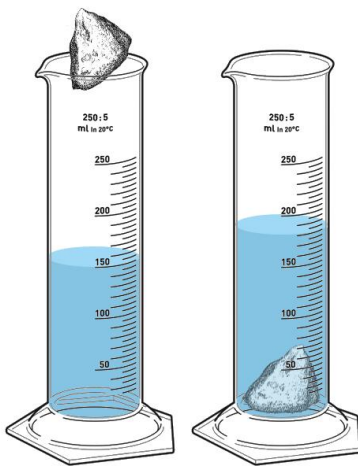


Figure 13: Diagram showing measurement by displacement. Image reuses public domain artwork from Lord Belbury, CC BY-SA 4.0 <<https://creativecommons.org/licenses/by-sa/4.0/>>, through Wikimedia Commons.

Before measuring the displaced volume, the ablation zone was debrided. This was done post-MRI with a chirurgic scalpel until the necrotised area was completely exposed. A 500 ml measuring cylinder was then filled to the brim and placed into an overflow container on a tared scale (**Figure 14a**). When the ablation was placed into the measuring cylinder (**Figure 14b**) water was displaced by its weight (**Figure 14c**). This water collected at the bottom of the overflow container. It was weighed and its mass equalled to the volume of the ablation (1 ml = 1 cm³).

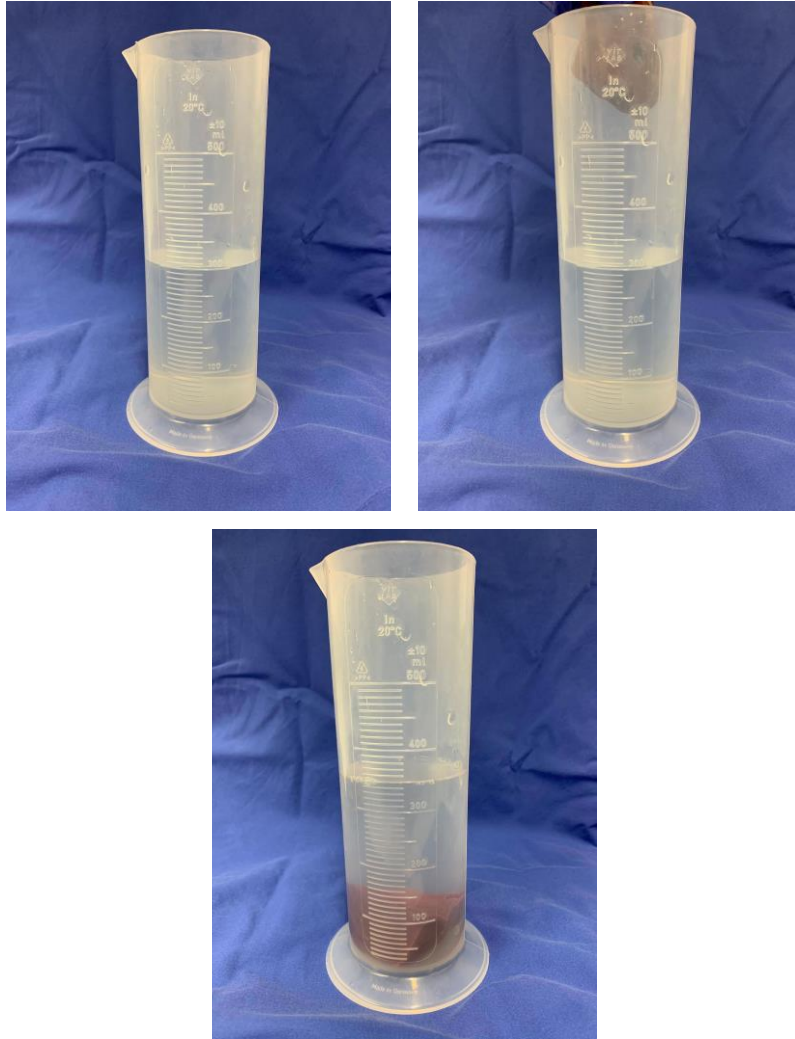


Figure 14. a) Initial volume of 300 ml before adding the liver ablation. b) Process of adding a stand-in piece of liver. c) Final volume of ca. 350 ml.

We followed Hemmerich et al.'s collective data set algorithm to determine a suitable statistical technique. Our main independent variable (IV) would be the type of applicator used: a stand-alone applicator system (S_N), a closed spacer-supported applicator system (S_C) and an open spacer-supported applicator system (S_O). Our secondary independent variable would be power input (W) and time interval (min) during laser ablation. Our dependent variables would be the ablation diameter (\emptyset) and the ablation volume (V). As the influence of every independent variable on every dependent variable would be observed we chose a within-subject design. As all dependent variables were physical measurements, we also chose a continuous scale for dependent variables. There was no need to control a covariate as every other variable was fixed (**Table 2**). It was also desirable to examine the two dependent variables in one unified analysis. Using this algorithm, a **one-way repeated measures multivariate analysis of variance (orMANOVA)** was chosen to be most suited to the data set. [74]

There are four main requirements for the implementation of an orMANOVA:

- I. Independence of measurements: Any measurement from one independent variable must not be influenced by a measurement from another independent variable. As the spacers act wholly independent of each other, this requirement is fulfilled.
- II. Measurement of DVs through a metric scale: As this dissertation utilises a metric scale entirely, this requirement is also fulfilled.
- III. Measurement of IVs through a nominal scale: In this case the IV is separated in three subgroups on a multinominal scale: S_C , S_O and S_N . This requirement is therefore also fulfilled.
- IV. Adequate sample size: Each measurement of DVs should be repeated a number of times which is greater or at least equal to the total amount of DVs. The process of laser ablation with each applicator type was

repeated 15 times, and the dependent variables were thus also measured 15 times (15 repetitions > 2 DVs).

Assessing the data set through orMANOVA allowed measuring the effect of the independent variables (spacer categories) on the dependent variables. Beyond that, it could also calculate whether that effect was statistically significant. Statistical significance was then determined by ascertaining Wilks' Lambda through orMANOVA.

REPRODUCTION RELIABILITY

As measuring ablation diameter was done manually with a millimetre ruler, the chance of random measurement errors occurring in those cases was higher than in the cases of MRI volumetry and displacement volumetry. Therefore, V_{MRI} and V_D were chosen to be investigated for internal consistency. There are several ways to observe test-retest reliability, but only two of them suit metric parameters: Pearson's r correlation and intraclass correlation coefficient (ICC). [75] As more than two "raters", or in this case test repetitions, were present, only ICC applied. ICC can be divided into several different forms based on the "model", "type" and "definition". For this trial Koo et al.'s standard formula of reporting was chosen as according to their flowchart outlined in 2016's *A Guideline of Selecting and Reporting Intraclass Correlation Coefficients for Reliability Research*. [76]

ICC estimates and their 95% confidence intervals were calculated using SPSS statistical package version 28 (SPSS Inc., Chicago, IL) based on a **mean-rating (k = 25), absolute-agreement, 2-way mixed-effects model**. Interpreting ICC is done through evaluating a number between 0 and 1. If the data set consists of identical values, ICC will be 1. In clinical settings it is agreed that an ICC above 0.7 is deemed acceptable, an ICC above 0.8 good and an ICC above 0.9 excellent in terms of test-retest reliability. Koo et al. recommend an ICC of at least 0.8 for clinical studies. It must be noted that the ICC calculated by SPSS is only an estimate, as the result depends heavily on the design of the study or the effect model chosen. For example, a one-way model will generally put out smaller estimates than a two-way model. [74, 76]

3 RESULTS

3.1 TIME INTERVAL AND POWER INPUT

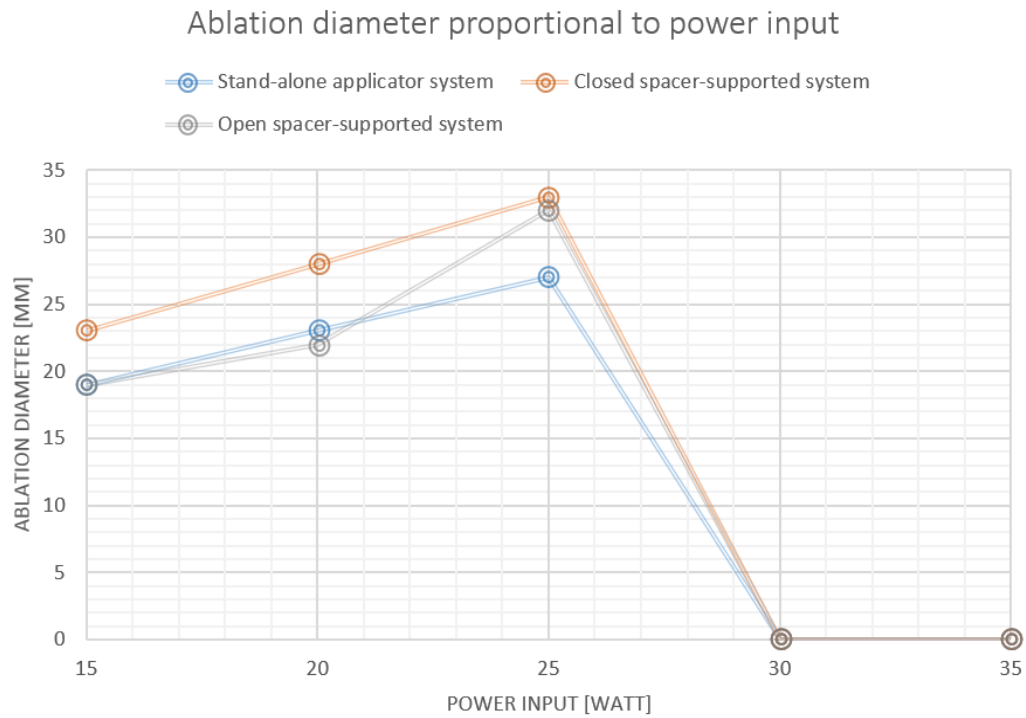


Figure 15: Ablation diameter [mm] proportional to power input [W].

The aim of the first trial was to establish the highest possible power input that could be set without carbonisation occurring. Fixed variables such as **time**, **perfusion flow**, **liver temperature**, **fluid temperature** and **insertion depth** were set to exclude covariates (**Table 2**). We then examined the influence of power input on the dependent variable ablation diameter.

	Value
Power input [W]	25
Time interval [min]	10
Perfusion flow [ml/h]	60
Liver temperature [°C]	37
Fluid temperature [°C]	20
Insertion depth [mm]	100
Tissue radius [mm]	100

Table 2: Fixed variables.

We started at a power input of 15 W and increased the power in increments of 5 W up to 35 W. **Ablation diameter** and the **presence of carbonisation** was measured. This experiment was in total repeated five times to avoid statistical measuring errors. Increasing the fixed variable **power** showed a proportional increase in ablation diameter. However (**Figure 15**) when the power was set to 30 W, tissue carbonisation occurred and the lasing process was aborted. This was the case in all five attempts at a power input of 30 W. Thus, it was concluded that **the maximum attainable power input without the presence of carbonisation was 25 W.**

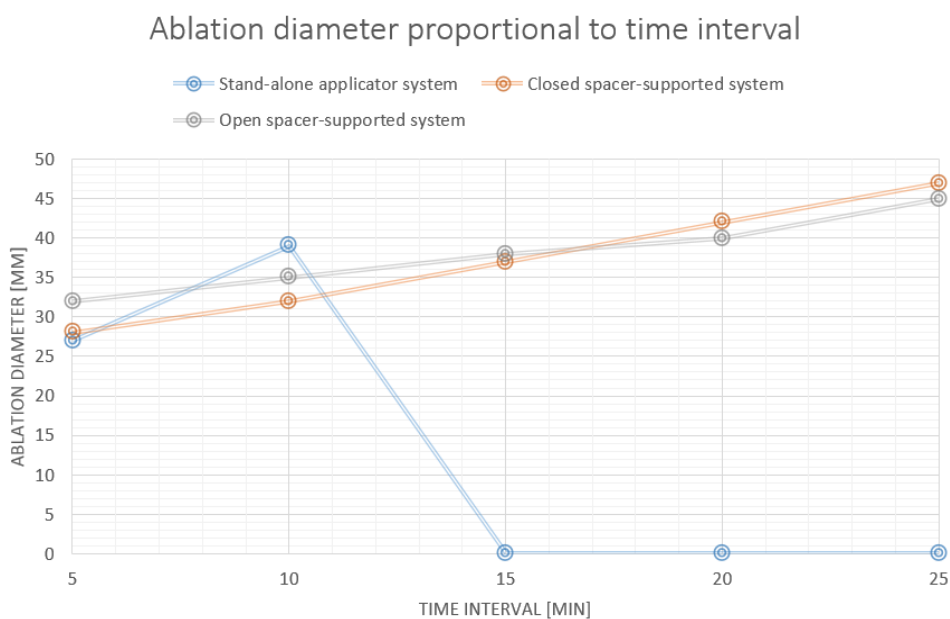


Figure 16: Ablation diameter [mm] proportional to time interval [min].

We now converted the previous independent variable of power input into a fixed variable of 25 W. The independent variable could thus be changed to the maximum **time interval** in which ablation was able to take place without carbonisation occurring. The previous fixed variables were kept (**Table 2**). Starting at a time limit of 5 min, the time was gradually increased by increments of 5 min to a total maximum of 25 min. Both **ablation diameter** and the **presence of carbonisation** was measured. We found that there was a positively proportional relationship between the time interval and ablation diameter for all three ablation types (see **Figure 16**). However, when using the stand-alone applicator system S_N the maximum time interval we could set was 10 min. When setting a time interval above 10 min the Lightguide Protection System (LPS) activated and the lasing process was aborted. We also found that carbonisation of central tissue and damage to the optical fibre had occurred when we dissected those ablation zones. LPS activation and thus carbonisation steadily occurred at a timeframe of $\Delta t = 10:11-12:03$ min. The constant LPS activation and carbonisation meant we were unable to record ablation diameter and volume at a longer time interval for S_N .

In contrast, we found that when using both spacers S_C and S_O the time interval was able to be extended to 25 min. No ablation zone showed carbonisation even at the maximum time of 25 min when we dissected them after volumetry.

To facilitate a comparison between all three applicator types S_N , S_C and S_O we chose a time interval of **10 min** was set. This interspacial trial allowed us to ascertain whether using a spacer – no matter which one – improved ablation size in comparison to not using one, and whether this increase was statistically significant. However, as the occurrence of carbonisation made it impossible to increase the time interval for the stand-alone applicator system beyond 10 min, we also conducted a second trial using only the spacer types S_C and S_O . This intraspacial trial was conducted using a time interval of 25 min.

3.2 REPRODUCTION RELIABILITY

The previous two experiments were conducted to determine the combination of maximum attainable time interval and power input which could be used without carbonisation occurring. Time interval and power input were then set as fixed variables.

We then repeated the ablation process using a stand-alone applicator system and the fixed variables of time interval = 10 min and power input = 25 min a total of 25 times. The ablation diameter measured during those 25 times was then used to compare the reliability of the recorded results given. Reliability will be defined as: *the extent to which measurements can be replicated*. [76] This was achieved through calculation of its test-retest reliability.

Reliability Statistics					
Cronbach's Alpha	N of Items				
0,855	2				

Intraclass Correlation Coefficient					
	Intraclass Correlation ^b	95% Confidence Interval		F Test with True Value	
		Lower Bound	Upper Bound	Value	df1
Single Measures	0,743 ^a	0,504	0,877	6,879	24
Average Measures	0,853 ^c	0,670	0,935	6,879	24

Intraclass Correlation Coefficient		
	F Test with True Value 0	
	df2	Sig
Single Measures	24	<0,001
Average Measures	24	<0,001

Two-way mixed effects model where people effects are random and measures effects are fixed.

- The estimator is the same, whether the interaction effect is present or not.
- Type A intraclass correlation coefficients using an absolute agreement definition.
- This estimate is computed assuming the interaction effect is absent, because it is not estimable otherwise.

Figure 17: Intraclass Correlation Coefficient and Cronbach's Alpha.

This data set of the ablation diameter calculated an average intraclass correlation coefficient of 0.85 (**Figure 17**). This indicated good reliability. Based on the 95% confidence interval of the average moderate to excellent reliability and internal consistency could be assumed. Cronbach Alpha, another measure of reliability, was calculated to be 0.85. This indicated good internal consistency.

3.2 INTERSPACIAL ABLATION SIZE

Utilising an exploratory data analysis it was determined that there were no univariate outliers in the data. The presence of multivariate outliers was evaluated by comparing the ideal Mahalanobis distance to the actual Mahalanobis distance. This depended on the number of dependent variables. As there were two dependent variables, a Mahalanobis distance above 13.82 meant the presence multivariate outliers. When calculating the Mahalanobis distance in this study the result was 9.83. It can therefore be concluded that there were no multivariate outliers in the data. [74] To avoid random measurement errors, each trial was conducted 15 times and the mean average of ablation diameter and ablation volume was calculated. This mean is abbreviated here for comparison and further statistical analysis (**Table 3**).

	S_N	S_C	S_O
\varnothing [mm]	37.60	28.67	31.00
V [cm ³]	23.61	18.12	18.49

Table 3: Mean ablation diameter and volume dependent on the applicator type.

When evaluating the effect the independent variable (applicator type) had on the dependent variables, we found that the ablation diameter and volume measured when using the stand-alone applicator system S_N were greater than those measured when using the closed spacer-supported system S_C or the open spacer-supported system S_O . This comparison is easily apparent in **Table 3**, as S_N has a mean diameter of 37.60 mm as opposed to the mean diameter of 28.67 mm when S_C was used. However to confirm the veracity of these results we also calculated the statistical significance of this difference.

Multivariate ^{a,b}						
Within Subjects Effect		Value	F	Hypothesis df	Error df	Sig.
spacer	Pillai's Trace	1,188	9,512	8,000	52,000	<0,001
	Wilks' Lambda	0,032	28,783 ^c	8,000	50,000	<0,001
	Hotelling's Trace	23,509	70,527	8,000	48,000	<0,001
	Roy's Largest Root	23,211	150,874 ^d	4,000	26,000	<0,001

- a. Design: Intercept
Within Subjects Design: spacer
- b. Tests are based on averaged variables.
- c. Exact statistic
- d. The statistic is an upper bound on F that yields a lower bound on the significance level.

Figure 18: Wilks' Lambda statistical significance test for interspacial comparison.

We first calculated the presence of significance by means of Wilks' Lambda through orMANOVA (**Figure 18**). The cut-off level of statistical significance was set to $p < 0.05$ with $\alpha = 0.05$. SPSS calculated Wilks' Lambda for the set dependent variables ablation diameter and ablation volume as $p < 0.001$. Thus we were able to conclude that there is a statistically significant effect the choice of applicator type had on ablation size.

Tests of Between-Subjects Effects							
Source	Dependent Variable	Type III Sum of Squares	df	Mean Square	F	Sig.	Partial Eta Squared
Spacer	Diameter	687,644	2	343,822	145,962	<0,001	0,874
	Volume	282,696	2	141,348	99,085	<0,001	0,825

Figure 19: Test of Between-Subjects Effects. Significance level set at $p < 0.05$.

As orMANOVA multivariate testing is an omnibus test, it is only able to ascertain *that* statistical significance is present when looking at all dependent variables combined. It cannot specify *which* dependent variables show a statistically significant difference. We conducted a test of between-subjects effects (**Figure 19**) through post-hoc univariate ANOVAs for both dependent variables. For both ablation diameter and ablation volume there was statistical significance:

$$\emptyset: F(2,42) = 148.735, p < 0.001, \text{partial } \eta^2 = 0.876$$

$$V: F(2,42) = 99.085, p < 0.001, \text{partial } \eta^2 = 0.825$$

The choice of spacer category therefore has a significant effect on **both** ablation diameter and ablation volume. There also was a significant difference between the three applicator types. However post-hoc univariate ANOVAs are limited in ascertaining the presence of statistical significance when looking at an individual dependent variable. They cannot explore the *qualitative* difference in each dependent variable depending on which applicator type was used. For that a pairwise comparison through post hoc Tukey and Games-Howell testing was employed.

Interspatial ablation diameter

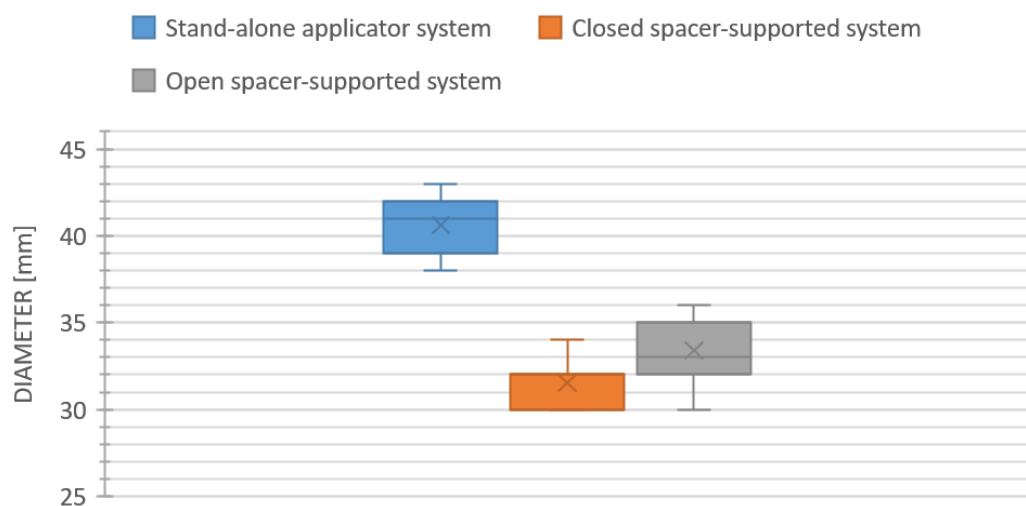


Figure 20: Interspatial ablation diameter [mm].

We found a statistically significant increase in ablation diameter and volume ($p < 0.001$) when comparing the stand-alone applicator system S_N to the closed spacer-supported system S_C (**Figure 20** and **Figure 21**). The mean difference was approximately 8.93 mm.

$$\emptyset: F(2,42) = p < 0.001, (M_{\text{Diff}} = 8.9333, 95\text{-CI}[7.6280, 10.2387])$$

$$V: F(2,42) = p < 0.001, (M_{\text{Diff}} = 5.4887, 95\text{-CI}[4.4291, 6.5482])$$

When comparing S_N to the open spacer-supported system S_O we also noted a statistically significant increase in ablation diameter and volume ($p < 0.001$).

\emptyset : $F(2,42) = p < 0.001$, ($M_{Diff} = 6.6000$, 95%-CI[5.2947, 7.9053])

V: $F(2,42) = p < 0.001$, ($M_{Diff} = 5.1267$, 95%-CI[4.0671, 6.1682])

Interspatial ablation volume

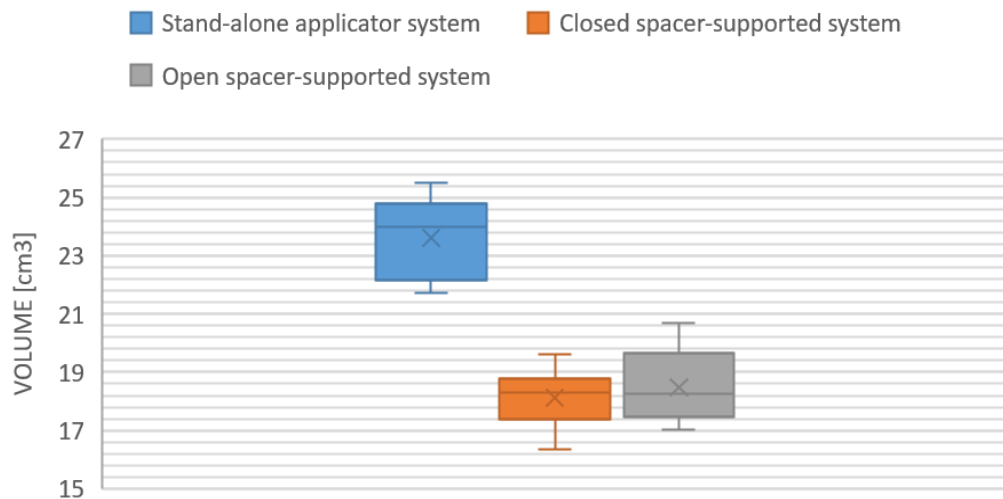


Figure 21: Interspatial ablation volume [cm³].

S_C and S_O showed no statistically significant difference when comparing ablation volume (Tukey HSD $p = 0.69$, Games-Howell $p = 0.63$). However, S_O 's ablation diameter was statistically significant in its increase to S_C :

\emptyset : $F(2,42) = p < 0.001$, ($M_{Diff} = 2.3333$, 95%-CI[1.0280, 3.3687])

We concluded that at a time interval of 10 min using a conventional stand-alone applicator system was superior to the use of a spacer, no matter whether open or closed. However as **3.1 Time Interval and Power Input** showed, the stand-alone applicator was unable to withstand a time interval beyond 10 min. **As such we aimed to assess ablation diameter and ablation volume when using a spacer-supported system at 25 min.**

3.3 INTRASPACIAL ABLATION SIZE

Our goal in this experiment was the comparison of ablation size between the two spacer variants at a time interval of 25 min. All other fixed variables (**Table 2**) remained the same. The ablation process was again repeated 15 times each with each spacer type. The dependent variables ablation diameter (\varnothing) and ablation volume (V) were recorded. We additionally performed a second exploratory data analysis, and determined that there were no univariate outliers in this data set as well. The Mahalanobis distance in this experiment was also 9.83 and as such there were no multivariate outliers. [74] The mean average of ablation diameter and ablation volume was calculated and is depicted in **Table 4**.

	S_c	S_o
\varnothing [mm]	52.07	47.60
V [cm ³]	75.25	72.20

Table 4: Mean diameter [mm] and volume [mm] for both the closed spacer (S_c) and the open spacer (S_o).

In **Table 4** we can see that there is also a difference in ablation diameter and volume between the two spacer types: S_c has both the larger ablation diameter and the bigger ablation volume. However, we did not yet appraise whether this difference was also statistically significant. For that we first determined the general presence of statistical significance by calculating Wilks' Lambda through orMANOVA. We set $p < 0.05$ again

Multivariate Tests^a

Effect		Value	F	Hypothesis df	Error df	Sig.	Partial Eta Squared	Noncent Parameter	Observed Power ^c
Intercept	Pillai's Trace	.999	11373.002 ^b	4.000	25.000	.000	.999	45492.009	1.000
	Wilks' Lambda	.001	11373.002 ^b	4.000	25.000	.000	.999	45492.009	1.000
	Hotelling's Trace	1819.680	11373.002 ^b	4.000	25.000	.000	.999	45492.009	1.000
	Roy's Largest Root	1819.680	11373.002 ^b	4.000	25.000	.000	.999	45492.009	1.000
Spacer	Pillai's Trace	.572	8.370 ^b	4.000	25.000	.000	.572	33.478	.995
	Wilks' Lambda	.428	8.370 ^b	4.000	25.000	.000	.572	33.478	.995
	Hotelling's Trace	1.339	8.370 ^b	4.000	25.000	.000	.572	33.478	.995
	Roy's Largest Root	1.339	8.370 ^b	4.000	25.000	.000	.572	33.478	.995

a. Design: Intercept + Spacer
b. Exact statistic
c. Computed using alpha = .05

Figure 22: Wilks' Lambda statistical significance test for intraspatial comparison.

When using SPSS we calculated (**Figure 22**) the Wilks' Lambda level of statistical significance at $p < 0.0005$. Thus, there is a statistically significant effect spacer subgroups have on \emptyset and V. Due to the existence of only two independent variables the test of between-subject effects through post hoc univariate ANOVAs could not be conducted. Therefore, it was not immediately clear whether there was a statistically significant difference for *both* dependent variables as the effect of the spacer type. As the Wilks' Lambda test only shows the existence of a statistically significant difference and does not indicate its quality, it was decided to proceed with a pairwise comparison through post hoc Tukey and Games-Howell testing.

Intraspatial ablation volume

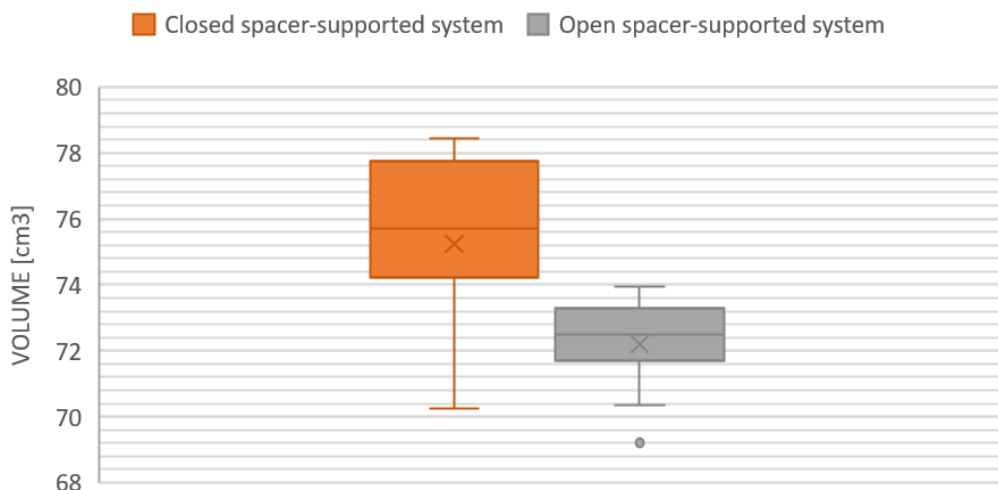


Figure 23: Intraspatial ablation volume [cm³].

After calculating the qualitative difference for every dependent variable through SPSS we found that there was statistical significance when comparing **ablation volume V** between the two spacer types (**Figure 23**). When using S_N we recorded a mean volume of $V = 75.25 \text{ cm}^3$. This was an increase in comparison to S_O , which had a mean of $V = 72.20 \text{ cm}^3$. The mean difference between S_C and S_O was $\Delta V_D = 3.05 \text{ cm}^3$. This difference was statistically significant to the point of $p < 0.001$:

$$F(2,42) = p < 0.001, (M_{\text{Diff}} = 3.0527, 95\text{-CI}[1.6121, 4.4932])$$

Intraspacial ablation diameter

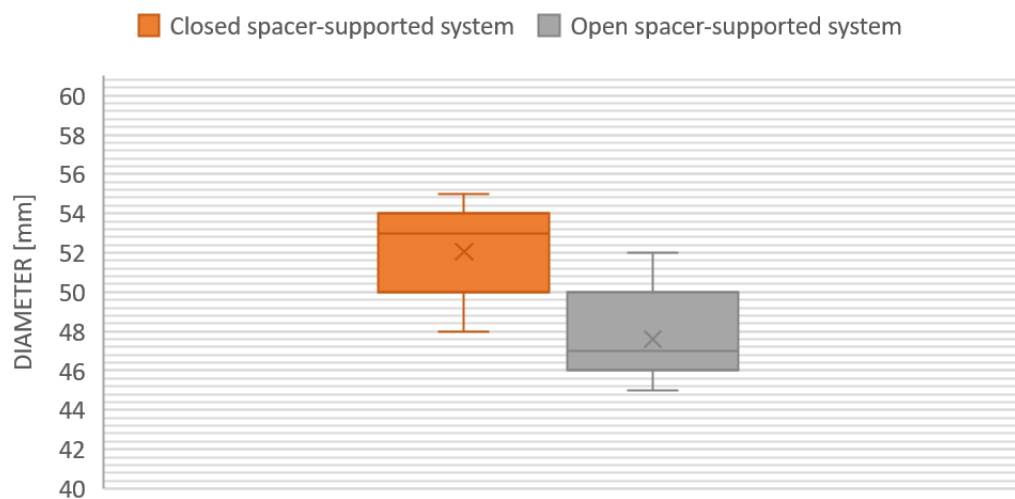


Figure 24: Intraspacial ablation diameter [mm].

For the dependent variable **ablation diameter \emptyset** we also found a statistically significant difference to the point of $p < 0.001$: When using S_C we recorded a mean diameter of $\emptyset = 52.067 \text{ mm}$, which was an increase to the diameter mean of $\emptyset = 47.60 \text{ mm}$ recorded when using S_O (**Figure 24**).

$$F(2,42) = p < 0.001, (M_{\text{Diff}} = 4.46667, 95\text{-CI}[2.6479, 6.2854])$$

On page 7 we discussed how previous studies and developments in ablation therapy offer little insight in how to treat lesions in the category of 30 – 50 mm. When

evaluating the data we derived from this experiment we can draw the conclusion that S_c reached this threshold of 50 mm ablation size in 12/15 cases (80%). In 3/15 cases it exceeded the threshold by ≥ 5 mm (20%), which is described by An et al. as a minimal tumour margin considered “safe” in ablation procedures. [36] S_o reached the threshold of 50 mm ablation size in 4/15 cases (26.67%). In 0/15 cases it exceeded the threshold by ≥ 5 mm (0%). We therefore derived two conclusions: 1) that when using the closed spacer-supported system we were able to reach 50mm ablation diameter; and 2) that both spacer-supported systems drastically improved upon ablation size in comparison to the stand-alone applicator system.

We will expand on this in the discussion.

Due to an increase in prevalence and incidence of cancerous disease, minimally invasive therapeutic options have been increasingly explored as a valid alternative or accompaniment to conventional treatment. One of those therapeutic options is the concept of thermal ablation. Thermal ablation has been reported as especially effective in the treatment of hepatic lesions, such as hepatocellular carcinoma and metastases. [56] Several ablation modalities such as radiofrequency, microwave and laser exist. Those modalities differ greatly in terms of biomechanics, indications, practicability and cost effectiveness. However, the main limitation of each modality remains its maximum ablation size. [77]

Smaller lesions measuring up to 30 mm diameter or 25 cm³ volume are able to be fully ablated when including a safe margin (> 5 mm) [77]. However, medium-sized lesions with a diameter of 30-50 mm are unable to be fully ablated with a singular applicator in a singular application. [14] Full ablation of tumours between 30-50 mm is currently only possible through multiple applicators, several rounds of applications and differing applicator positioning, or the combination of surgical and interventional techniques such as combining vascular clamping with an ablation modality. [25–27] Vascular clamping of the total, partial or selective hepatic flow is a valid method. However, it is technically demanding, shows association to intestinal congestion and requires an intermittent or continuous period of organ ischemia. [61, 78]

Ablation size limitation in thermal ablation is caused by overheating near the applicator. Once tissue temperature reaches > 100°C vital heat-conducting tissue transforms into a nonconductive boundary layer. This boundary layer acts as an insulating “shell” which limits further energy transmission into peripheral tissue. In radiofrequency ablation abrupt changes in tissue impedance have been reported to create “heat spots” around the probes. [79] In microwave ablation and laser ablation the formation of a boundary layer around the applicator has been described as “carbonisation”. [80] In laser ablation this carbonisation also causes damage to the

optical fibre through central overheating, a process in which the ablation procedure is automatically aborted through a Lightguide Protection System. [81]

Preventing carbonisation has been key in increasing ablation size, as several developments in recent years show: For microwave ablation in recent years an internal cooling jacket has been developed. [82] Radiofrequency ablation and laser ablation have been improved through standardised development of cooling diffusers. [24, 83, 84] These improvements share similar aims and methods; their goal is the increase of energy diffusion through the targeted tissue by decreasing the temperature immediately adjacent to the heat source.

A technically comparatively simple and cost-effective approach to prevent carbonisation is the usage of a spacer. A spacer creates an artificial, fluid-filled space between the stand-alone applicator and the targeted, vital tissue. Our hypothesis was that the presence of a spacer would delay carbonisation or even prevent it entirely, and subsequently increase ablation size. We thus aimed to compare ablation size measured when using a spacer to ablation size measured when using the stand-alone applicator system. For that, two spacer types were developed: 1) a spacer with a closed tip where cooling fluid would circulate inside the applicator system and 2) a spacer with an open tip where cooling fluid would diffuse into the tissue. We measured ablation diameter and ablation volume in an ex vivo bovine model using a stand-alone laser applicator. The measurements were recorded through displacement volumetry and MRI volumetry. These recorded parameters were then compared to ablation diameter and ablation volume measured when using a closed spacer or an open spacer in laser ablation.

We also aimed to exclude covariates by setting fixed variables. For that, two pre-trials with all three applicator types were conducted. We first set a time interval of 10 min and compared ablation diameter with varying power inputs. We found that setting power input > 25 W would lead to almost instantaneous abortion of the ablation process due to central overheating. This happened both when the stand-alone applicator system was used and when the spacers were used. Conversely, low power such as 5 W or 10 W would allow longer ablation time intervals, but ultimately resulted

in smaller ablation size. We thus selected a power input of 25 W. With this power input fixed we then changed the time interval. For the stand-alone applicator system S_N any time interval of > 10 min would result in central overheating, carbonisation and abortion of the procedure. However, this was not the case for the closed spacer-supported applicator system S_C and the open spacer-supported system S_O . The spacers tolerated time intervals of up to 25 min.

These pre-trials allowed us to determine the fixed variables of power input and time interval which would maximise ablation diameter and volume while minimising chance of carbonation.

We then conducted our main two trials comparing the three applicator types. At a time interval of 10 min, we found that the stand-alone applicator system produced larger ablation diameter and ablation volume than both spacer-supported systems. This difference was statistically significant ($p < 0.001$) for both diameter and volume. However the limited time interval of 10 min prevented an accurate assessment of the spacer's possibilities. Our second main trial therefore compared ablation diameter and ablation volume of the two spacer types at a time interval of 25 min.

We found that the closed spacer-supported system was able to attain a mean ablation diameter of 54.13 mm and mean ablation volume of 75.29 cm^3 . When compared to the open spacer system with a mean ablation diameter of 47.60 mm and a mean ablation volume of 72.15 cm^3 this comparative increase was also statistically significant ($p < 0.001$) for both diameter and volume.

Additionally, we calculated the factor of change for ablation volume. This was achieved by comparing mean ablation volume of both spacer types to the stand-alone applicator system:

$$\frac{S_C \text{ ablation volume}}{S_N \text{ ablation volume}} = \frac{75.29}{23.61} \text{ cm}^3 = 3.19$$

$$\frac{S_O \text{ ablation volume}}{S_N \text{ ablation volume}} = \frac{72.15}{23.61} \text{ cm}^3 = 3.06$$

When using this factor of change we can derive that the increase in ablation volume was more than 300 % when a spacer was used as opposed to when no spacer was used. The validity of this derivation will be discussed in **4.4 Intraspatial Comparison**.

In conclusion, the objectives of this study have been fulfilled.

4.1 SPACER

The spacer developed by Prof. Dr. rer. nat. U.S. and Dr. med. vet. O.G. consists of a glass body and polypropylene tip. During critical evaluation of the spacer it should be discussed whether the material glass is suited for thermal ablation. In an ex vivo model a damaged spacer would mean the cancellation of the experiment; however in a clinical setting shattered glass inside of a patient's body would pose the possibility of haemorrhage as well as of infection. However, the glass body of the spacer is fashioned from a Pasteur pipette made out of borosilicate glass. Borosilicate glass is developed specifically for laboratory use and is able to withstand 200-230°C for standard-use service. Its thermal shock resistance, i.e. its resistance to glass temperature changing rapidly, is approximately 160°C. [85] In none of the trials the temperature measured exceeded 110°C. The maximum temperature change could be thus calculated to about 90°C:

$$\Delta T = (T_{\max} - T_{\text{fluid}}) = (110 - 20)^{\circ}\text{C} = 90^{\circ}\text{C}$$

In conclusion both maximum temperature and thermal shock index remain below the threshold needed for the spacer body to shatter. As such, the glass body is suitable for thermal ablation in pre-clinical trials. For clinical trialling the material should be adapted accordingly.

Second, the spacer body's diameter (\varnothing 4 mm) and wall thickness (\varnothing 0.5 mm) were arbitrarily chosen due to utilisation of a standard Pasteur pipette. At this point in time there is no data on whether the wall thickness might impact the spacer's effectiveness. However, it is entirely possible that a thinner spacer body would allow a more effective transmission of energy. Further evidence is needed before conclusions

can be drawn. Replacing the glass body with a further heat-resistant plastic material such as polydicyclopentadiene (PDCPD) and modifying its wall thickness could allow for an increase efficiency. The choice of material is subject to further discussion in 5

Conclusion and Outlook.

Third, the plastic tip was fashioned from an Eppendorf epT.I.P.S.[®] 200 μ l pipette tip. This specific tip is made out of polypropylene (PP), a heat-resistant material. The manufacturer (Eppendorf SE, Hamburg, Germany) notes that autoclaving of these pipette tips is possible at 121 °C for up to 20 min without damage. As such, the material of the pipette tip does not pose a primary technical disadvantage. However, it must be noted that the manufacturer recommends a maximum of a single autoclaving cycle and does not recommend reusing the pipette tips. During our study spacers were re-used for up to five times. There is no evidence that this causes the tip to be inherently unsuitable. The manufacturer merely states that “prolonged use **can** have a negative impact on dispensing tasks”. [86] However the inevitable wear and tear from both mechanical and thermal damage might eventually degrade the polypropylene. We did not note any macroscopic damage to the pipette tip, however microscopic plastic damage cannot be safely excluded.

Fourth, the weak point of the spacer was its proximal and distal junctures. Four closed spacer prototypes and three open spacer prototypes ($n = 7$) were manufactured. In case of a spacer breaking during the ablation process the trial was aborted and the location of the fracture was examined. In $n = 5$ cases those spacers had experienced fracture of the glass. The proximal vulnerable point was the glass body’s connection point to the Y connector. The UV-glued juncture would either disconnect, or the glass itself would fracture just distally of the glass body-Y connector junction. The distal vulnerable point was the glass body’s connection to the pipette tip. Interestingly enough, the pipette tip itself was not dislodged through weakening of the UV glue, which shows the heat stability of the glue’s properties, but the glass would fracture just proximally of the glass body-pipette tip junction. Each spacer was utilised up to five times to reduce the thermal stress and damage its material would undergo. It was observed that spacers would withstand being used up to five times, but would eventually break down. However, this does not indicate a general lack of suitability of

the spacer in thermal ablation. In a clinical setting, each standard applicator is only used a single time. This is regulated according to hygiene and structural concerns. As such, when possibly utilising a single-use spacer in future clinical trials, the spacer will not have experienced structural microdamage. In conclusion, the possible fracture points can be regarded as a side-effect of frequent use and are not applicable in a clinical setting.

4.2 SETTING

We will now evaluate the setting in which our study was performed.

First, we will assess the suitability of the tissue in which the ablation was performed. Human and bovine liver tissue are comparatively similar when examined histologically. Both are macroscopically covered by a thin hepatic capsule and divided into left and right lobes as well as a caudate and quadrate lobe. Its microscopic appearance also is similar: both human and bovine hepatic parenchyma is organised into lobules around central veins and bordered by a portal vascular triad. Differences include larger endothelial pores (so-called fenestrae) in human liver capillaries as well as higher sinusoid volume fraction in human tissue when compared to bovine. [87] As such, it cannot be definitively excluded that thermal ablation in human liver tissue would produce different results. However, Estermann et al. report that as opposed to porcine liver, bovine liver and human liver share close mechanical tissue properties due to similar collagen content. Additionally, contrary to porcine liver, bovine liver does not possess deep interlobar fissures which limit heat diffusion. The amount of fibre tissue connecting the lobes is much smaller in bovine liver than in porcine liver. Estermann et al. thus recommend that “for applications that require accurate elastic properties, possibly in the context of testing new medical devices, bovine liver should be used”. [88]

Secondly, we must discuss the natural physiological processes occurring during in vivo laser ablation. One of the most important influencing factors as well as a limitation in thermal ablation is the heat sink effect. This effect describes the reduction in ablation size occurring through diverting vessels such as larger veins. The constant circulating blood stream decreases tissue temperatures. Fei et al. note that the heat conductivity of blood is about five times higher than the conductivity of hepatic tissue. This results in heat diffusing through vascular diversion. [89] Livers in an ex vivo setting naturally experience no heat sink effect. It could be speculated that these ablation shapes are, as such, idealised ellipsoids. To go further, their diameters and volumes might be artificially amplified. This could be due to the ideal absorption of heat in ex

vivo tissue without the heat sink effect. Mensel et al. conducted a comparative study in 2005 with the aim of observing the effects of laser ablation in central hepatic tumours as opposed to peripheral hepatic tumours. They report an overall efficiency rate of 82.1% in ablating tumours adjacent to large vessels. This suggests that even though the heat sink effect might be considered as an influence, it does not wholly undermine the chance of successful ablation. [90] Additionally, Wacker et al. suggest temporarily disrupting hepatic arterial flow to enhance hepatic ablation. [91] In an unpublished study by Hosten et al. provided to the author, portal vein occlusion followed by either laser ablation or radiofrequency ablation lead to an increase in temperature measured by MR monitoring and subsequently to larger ablation size. [92] In the future, a similar experiment through balloon-guided occlusion of the main hepatic artery might be considered, similarly to how a balloon catheter is used in the carotid arteries during neuroradiological interventions.

Thirdly, there were no standardised guidelines on the setting of fixed variables. For example, the flow rate was set at 60 ml/h. There are little to no studies that centre on the ideal perfusion flow rate during laser ablation and none of them deal with clinical cases. Two publications only mention experimenting with ex vivo flow rates in passing. Vogl et al. note that increasing the perfusion flow rate from 40 ml/h to 60 ml/h did not result in further increase of ablation diameter, whereas setting it to less than 40 ml/h caused significantly faster carbonisation. [28] Roesler et al. did not report a significant increase in ablation size when increasing the flow rate from 45 ml/h to 90 ml/h. [93] Vogl et al. also suggest using aqua destillata, while Roesler et al. consistently use standard saline solution. When comparing the two in a side experiment, no statistically significant difference in ablation size between ablations perfused with aqua destillata and with standard 0.9% saline solution was found. Therefore the change of flow rate is subject to further discussion. The author suggests a follow-up study where, for example, a comparison between 30 ml/h, 60 ml/h and 90 ml/h saline solution and aqua destillata could be manufactured.

4.3 VOLUMETRY

The displacement volumetry was conducted through the manual enucleation of the hepatic ablation tissue through scalpel. Afterwards the displaced water was weighed by means of a collection receptacle. Manual errors could have been conducted here. First, the enucleation was completed until the first layer of ablation with partially vital tissue was visible. It must follow that it's possible that too much or too little tissue was resected in the process. At times, the distinction between partially vital tissue and fully necrotised tissue was minimal by visual judgement alone. Due to the hardened viscosity of the necrotised tissue manual enucleation was complicated. In cases where a cut into the tissue was enlarged through manual causation, the scalpel was withdrawn and the dissected tissue flap was re-attached to the ablation through a thin layer of superglue. When weighing the amount of glue utilised, it amounted to <1g. As such it was not a significant contribution in extra weight, and thus displacement volume. On the other hand, in some cases fully vital tissue borders were attached to larger partitions of ablation and coagulation. In these cases, resection was implemented as close to the necrotised tissue as achievable. In $n = 2$ cases complete resection was unable to be achieved. The resection border between fully vital tissue and partially vital tissue remained <1 mm. When calculating the additional volume this would add to the displacement an ellipsoid shape was assumed. Following Vogl et al.'s manual volume calculations the formula utilised was a standard $V = \frac{4}{3} abc$ volume formula bounded by the ellipsoid, with principal diameters $a b c$ comprising the length, width and breadth of the ablation zone. [16] In both cases the additional vital tissue border was calculated to be <0.1 cm³, which comprised approximately 0.1% of the total tissue volume ($V_1 = 73.53 \text{ cm}^3$, $V_2 = 77.73 \text{ cm}^3$). After statistical discussion this possibly false positive percentage was deemed as no hindrance to ascertaining accurate volumetric data.

As a comparison to the manual displacement volumetry, MRI-guided volumetry through Horos DICOM viewer program was completed. Horos has been noted for its accuracy and confidence in determining both pre- and postoperative tumour volume.

Elsawaf describes it as a “highly effective mean of volumetric analysis”. [94] Through closed-polygon tooling of the MRI-recorded ablation in T2 FLAIR sequencing “region of interest” (ROI) points are created. Horos has the added benefit of the “Generate Missing ROIs” function. This function identifies possible missing ROI points through an artificially intelligent recognition pattern after a certain number of images in the sequence have been measured manually. ROIs that closely match the manually selected polygon borders are automatically created and are subject to manual review before a volumetric assessment is completed. It is also possible to create a 3D model of the ROI for visual purposes. As the initial closed-polygon tooling is done manually, it is possible to manually mismeasure the border between the ablation zone and vital tissue. As a consequential error the program might misidentify ablation zones through the “Generate Missing ROIs” function and create false ROI points. To avoid this, multiple test ROIs were created before measuring and recording the experiment’s ablation volumes. These manual and automatic volumetry results were compared with each other and showed no statistically significant difference (mean $\Delta V_{MRI} = 0.089 \text{ cm}^3$). It was thus concluded that the manual generation of ablation volume and the automatic assessment through artificial intelligence was closely similar.

When comparing the two methods of displacement volumetry and MRI volumetry an unpaired t-test was employed. As opposed to a paired t-test an unpaired t-test is based on the assumption that both dependent variables are not related to each other (for example, the comparison of a treatment group to a control group). Paired t-tests are considered more powerful when determining statistical significance, but require a close relation between the dependent variables (for example, measuring a variable before and after an event in the same group). Unpaired t-tests were calculated for every V_{MRI} and V_D pair in the interspacial and intraspacial trial (**Table 5**). The two-tailed P value was set at 0.05. Values > 0.05 were considered not statistically significant.

Two-tailed P value $V_{MRI} \leftrightarrow V_D$	Mean Δ	95% CI Δ
--	---------------	-----------------

Interspatial S _N	0.9228	-0.0507	-1.1126 - 1.0112
Interspatial S _C	0.1216	0.5507	-0.1558 - 1.2572
Interspatial S _O	0.1302	0.6327	-0.1985 - 1.4638
Intraspatial S _C	0.9400	0.0687	-1.7832 - 1.9206
Intraspatial S _O	0.8328	-0.1040	-1.1035 - 0.8955

Table 5: Calculated P-value between V_{MRI} and V_D

In both the interspatial and intraspatial trials the two-tailed P value was consistently >0.05. Thus there was no statistically significant difference between the measuring of displacement volume and the measuring of MRI volumetry.

4.4 INTRASPACIAL COMPARISON

The interspacial and intraspacial trial are based on different foundations of comparative approach. When comparing the three applicator types S_N , S_C and S_O utilised as independent variables it could be questioned whether the interspacial and intraspacial trial can be compared with each other in the first place.

For the first interspacial trial with the time limit of 10 minutes and power of 25W, the standard applicator system with no spacer performed better both in terms of ablation size and volume. For both dependent variables S_N showed a statistically significant positive difference when compared to S_C and S_O . It could be concluded that for smaller ablation sizes up to 30 mm in ablation diameter or 20 cm³ in volume the standard applicator system is preferable. However, the stand-alone applicator was unable to ablate beyond a time interval of 10 minutes. Central tissue temperatures increased exponentially and carbonisation occurred. It is impossible to differentiate whether S_N 's performance would have compared positively or negatively at a higher time interval. As such, the hypothesis that S_N 's comparatively better performance in the *interspacial* trial would equal comparatively better performance in the *intraspacial* trial is based on logical fallacy. The intraspacial trial must be observed independently and without comparison to S_N 's results in the interspacial trial.

When assessing the intraspacial trial through MRI T2 FLAIR imaging several differences are apparent: First, the border between ablation and vital tissue/partially vital tissue can be decidedly differentiated in the MRI imaging of the closed spacer (**Figure 25a**). It is more difficult to do so in the MRI imaging of the open spacer (**Figure 25b**). The border in **Figure 25b** appears spongiose and diffuse and due to the diffusion of fluid it is partially disseminated. Second, through fluid diffusion the overall size of the ablation is decreased: wherein **Figure 25a** features a solid ellipsoid sphere of ablation with clearly ablated tissue, **Figure 25b** features several fluid pockets inside of the ablation. Both hyperintense and hypointense spaces around the fluid pockets are present, pointing towards only partially ablated tissue. Finally, when comparing

ablation diameter and volume, S_c features larger relative ablation diameter and volume when measured by both MRI and displacement volumetry.

In summary, the open spacer seems to at first perform negatively when compared to the closed spacer. However, the open spacer also opens up several possibilities. In this trial, regular saline solution as well as aqua destillata were used for perfusion. As seen in **Figure 25a** there is no extraneous fluid within the ablation zone or the vital tissue. **Figure 25b** shows that the perfused tissue displayed a comparatively even spread of fluid pockets in both the tissue-ablation border and the vital tissue. This indicates that the fluid moved evenly through the vital tissue but was not able to form fluid pockets in areas where ablation has fully been completed. Peripherally from the ablation zone the fluid pockets decrease in size, with the largest pockets found right near the border between ablated tissue and vital tissue.

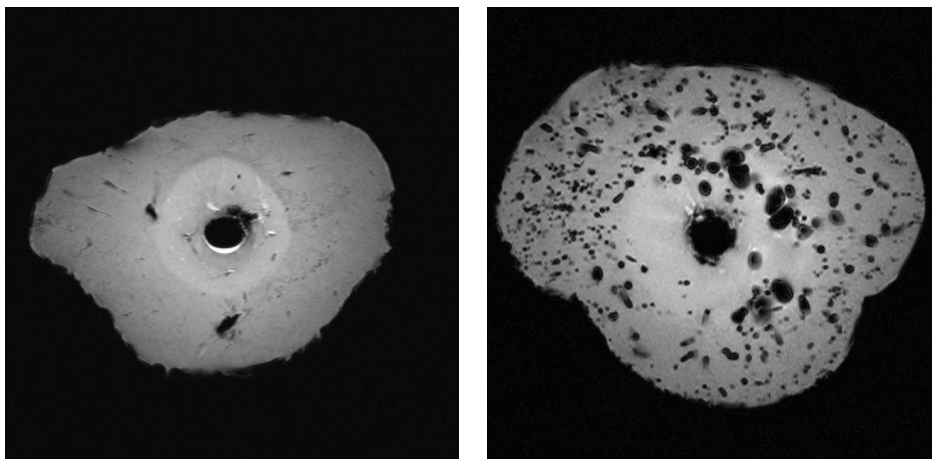


Figure 25: a) Tissue-fluid distribution within the closed spacer-supported ablation system. b) Tissue-fluid distribution within the open spacer-supported ablation system.

This leads to the hypothesis that if another type of fluid was used, the spread of this fluid into nearby tissue might lead to fluid-tissue interactions. This is very similar to another type of tumour ablation: trans-arterial chemoembolization (TACE). Vogl et al. define TACE as the “selective regional application of a chemotherapeutic substance with subsequent occlusion”. [95] Several embolization materials such as Lipiodol, gelatine sponges or Gelfoam are used in combination with cytotoxic agents. Doxorubicin is one of the most common substances used in TACE. This is due to its

adaptability in combination with the embolization materials. Butt et al. found that the combination of low-dose adjuvant doxorubicin and laser ablation lead to a statistically significant improved rate of overall survival when compared to bevacizumab or standard chemotherapy. [96] However, this was based on intravenous application of doxorubicin. Pacella et al. conducted study on large palliative-care HCCs with no possibility of surgical treatment. They observed the effectiveness of LA/TACE combination with doxorubicin. Total tumour ablation was achieved in 97% of cases, with a 3-year recurrence rate of 7%. With a mean tumour diameter of 52 mm, this study shows comparable similarities to research cited in this dissertation. Pacella describes injecting “10 mL of iodized oil, 20 mg of doxorubicin hydrochloride dissolved in 5 mL of distilled water (4 mg/mL), and radiologic contrast material (iopromide in water solution) in a final volume of 30 ml.” [97] Pacella does not describe the flow rate in which the volume was administered and the study differs in that TACE was performed 30-90 days after initial laser ablation. He offers no explanation for that, but it is plausible that a delay was set to monitor liver function and reduce post-LA hepatic oedema before TACE.

In none of the studies who report a LA/TACE combination therapy of hepatic tumour tissue the possibility of a simultaneous application of both thermal ablation and chemical ablation is mentioned. However, when considering the options of the open-ended spacer a replacement of the saline solution or aqua destillata used in this trial with the doxorubicin blend used by Pacella seems feasible. It is clear that further studies using the open spacer are needed to further the hypothesis that a simultaneous usage of doxorubicin-guided laser ablation and trans-arterial chemoembolization is possible. Due to doxorubicin’s vivid red colouring, an ex vivo trial using the open spacer could provide further evidential information on the diffusion spread through hepatic tissue. Such a trial could be attempted in the future.

This cumulative dissertation is a preliminary *proof of concept* study exploring the impact of a spacer on thermal ablation size. We found that the presence of a spacer between applicator and tissue did not only delay carbonisation, it also increased the attainable ablation volume by a factor of change of more than 300 %. Our findings were accepted for publication in February 2023 and published in *Biomedicines*. [43] However, the study's limitations include the *ex vivo* setting and use of bovine healthy liver. Additionally, the spacer's material at this point in time are not suitable for the requirements of both patients and medical providers. The usage in clinical practice requires further development as well as the conduct of additional pre-clinical studies.

In future work the author plans to expand on this spacer prototype. This might be accomplished by altering the materials used, such as using a heat-resistant material like polydicyclopentadiene. PDCPD is noted by Chen et al. to withstand temperatures up to 200°C when crosslinked. [98] The author anticipates that rising prevalence of 3D printing for both medical and experimental use in the last decade will also lead to new explorable avenues. Gross et al. refer to 3D printing as “an ideal rapid fabrication technique for small-scale or scalable applications given the array of available materials that can be printed”. [99] Using a 3D printing process to manufacture custom spacers would allow a wide array of materials to be used, as well as alterations to the spacer itself. If, for example, the spacer's wall thickness might be modified through custom 3D printing, its impact on ablation size and volume could lead to further developments. Another opportunity would be the use of heat-resistant fabric such as Gore-Tex® for designing an inflatable spacer. Gore-Tex® has been increasingly used in diverse medical settings, for example as material for gastrostomy tubes [100] or intravenous cannulas. [101]

Laser ablation can be considered optimal for preclinical studies, yet also performs worse in terms of ablation size when compared to radiofrequency ablation and microwave ablation. [102–104] Radiofrequency ablation is deemed a standard

staple in minimally invasive tumour therapy, yet also has several limitations: multiple probes cannot be used due to electromagnetic interference, its heating patterns are more heterogenous and unpredictable compared to microwave ablation, and the presence of grounding pads increases the risk of periprocedural burns. [105]

Microwave ablation is noted as the most suitable candidate for further development. Even at its stage of continued technical development and comparative newness it has proven to produce promising ablation sizes. [78] Higher intratumoral temperatures are considered its main disadvantage. Subsequently, further development of a method to circumvent those temperature spikes has been studied in recent years. [106]

Observing the influence of a spacer's presence in microwave ablation and its impact on tissue temperature and ablation size is a natural next step. A spacer constructed for usage in microwave ablation would necessarily be composed of heat-resistant, highly conductive materials with low absorption. [107, 108] Before the utilisation of the spacer in clinical practice is realised, further evaluation of its efficacy and safety is needed. This may be accomplished by means of continued preclinical studies on in vivo models. In closing the author concludes that spacer-supported thermal ablation is a viable option to be developed further.

- 1 Bertz J, Dahm S, Haberland J et al. **Verbreitung von Krebserkrankungen in Deutschland.** *Robert-Koch-Institut.* 2010: 156–172. DOI: 10.25646/3151
- 2 Oshowo A, Gillams A, Harrison E et al. **Comparison of resection and radiofrequency ablation for treatment of solitary colorectal liver metastases.** *Br J Surg.* 2003: 1240–1243. DOI: 10.1002/bjs.4264
- 3 Weis S, Franke A, Mössner J et al. **Radiofrequency (thermal) ablation versus no intervention or other interventions for hepatocellular carcinoma.** *Cochrane Database Syst Rev.* 2013: CD003046. DOI: 10.1002/14651858.CD003046.pub3
- 4 Vogl TJ, Mack MG, Müller PK et al. **Interventional MR: interstitial therapy.** *European radiology.* 1999: 1479–1487. DOI: 10.1007/s003300050874
- 5 Sharma DN, Thulkar S, Kumar R et al. **Interstitial brachytherapy for liver metastases and assessment of response by positron emission tomography: a case report.** *J Contemp Brachytherapy.* 2010: 114–116. DOI: 10.5114/jcb.2010.16922
- 6 Llovet JM, Bruix J. **Systematic review of randomized trials for unresectable hepatocellular carcinoma: Chemoembolization improves survival.** *Hepatology.* 2003: 429–442. DOI: 10.1053/jhep.2003.50047
- 7 Kwak MH, Lee MW, Ko SE et al. **Laparoscopic radiofrequency ablation versus percutaneous radiofrequency ablation for subphrenic hepatocellular carcinoma.** *Ultrasonography.* 2022: 543–552. DOI: 10.14366/usg.21241
- 8 Ferrari FS, Megliola A, Scorzelli A et al. **Treatment of small HCC through radiofrequency ablation and laser ablation. Comparison of techniques and long-term results.** *Radiol Med.* 2007: 377–393. DOI: 10.1007/s11547-007-0148-2
- 9 Buell JF, Thomas MT, Rudich S et al. **Experience with more than 500 minimally invasive hepatic procedures.** *Ann Surg.* 2008: 475–486. DOI: 10.1097/SLA.0b013e318185e647

-
- 10 Rhim H, Lim HK. **Radiofrequency ablation of hepatocellular carcinoma: pros and cons.** *Gut Liver.* 2010: S113-8. DOI: 10.5009/gnl.2010.4.S1.S113
 - 11 Li D, Kang J, Golas BJ et al. **Minimally invasive local therapies for liver cancer.** *Cancer Biol Med.* 2014: 217–236. DOI: 10.7497/j.issn.2095-3941.2014.04.001
 - 12 Brace C. **Thermal tumor ablation in clinical use.** *IEEE Pulse.* 2011: 28–38. DOI: 10.1109/MPUL.2011.942603
 - 13 Bucknor MD, Beroukhim G, Rieke V et al. **The impact of technical parameters on ablation volume during MR-guided focused ultrasound of desmoid tumors.** *Int J Hyperthermia.* 2019: 473–476. DOI: 10.1080/02656736.2019.1590654
 - 14 Lucatelli P. **Ablation: Is There Still Room For Improvement?** *ECIO 2022.* Lucatelli P. 2022. Im Internet: library.cirse.org/ecio2022/crs/101-3-ablation-is-there-still-room-for-improvement
 - 15 Vogl TJ, Straub R, Eichler K et al. **Malignant liver tumors treated with MR imaging-guided laser-induced thermotherapy: experience with complications in 899 patients (2,520 lesions).** *Radiology.* 2002: 367–377. DOI: 10.1148/radiol.2252011171
 - 16 Vogl TJ, Naguib NNN, Eichler K et al. **Volumetric evaluation of liver metastases after thermal ablation: long-term results following MR-guided laser-induced thermotherapy.** *Radiology.* 2008: 865–871. DOI: 10.1148/radiol.2491072079
 - 17 Heisterkamp J, van Hillegersberg R, Ijzermans JN. **Interstitial laser coagulation for hepatic tumours.** *Br J Surg.* 1999: 293–304. DOI: 10.1046/j.1365-2168.1999.01059.x
 - 18 Stureson C. **Interstitial laser-induced thermotherapy: Influence of carbonization on lesion size.** *Lasers Surg. Med.* 1998: 51–57. DOI: 10.1002/(SICI)1096-9101(1998)22:1<51::AID-LSM12>3.0.CO;2-B
 - 19 Hong K, Georgiades C. **Radiofrequency ablation: mechanism of action and devices.** *J Vasc Interv Radiol.* 2010: S179-86. DOI: 10.1016/j.jvir.2010.04.008

-
- 20 Rhim H, Goldberg SN, Dodd GD et al. **Essential techniques for successful radio-frequency thermal ablation of malignant hepatic tumors.** *Radiographics*. 2001: S17-35; discussion S36-9. DOI: 10.1148/radiographics.21.suppl_1.g01oc11s17
- 21 Gough-Palmer AL, Gedroyc WMW. **Laser ablation of hepatocellular carcinoma--a review.** *World J Gastroenterol*. 2008: 7170–7174. DOI: 10.3748/wjg.14.7170
- 22 Germer C-T, Roggan A, Ritz JP et al. **Optical properties of native and coagulated human liver tissue and liver metastases in the near infrared range.** *Lasers Surg Med*. 1998: 194–203. DOI: 10.1002/(SICI)1096-9101(1998)23:4<194::AID-LSM2>3.0.CO;2-6
- 23 Poch FGM, Neizert CA, Geyer B et al. **Perivascular vital cells in the ablation center after multibipolar radiofrequency ablation in an in vivo porcine model.** *Sci Rep*. 2021: 13886. DOI: 10.1038/s41598-021-93406-2
- 24 Hosten N, Stier A, Weigel C et al. **Laser-induzierte Thermotherapie (LITT) von Lungenmetastasen: Beschreibung eines miniaturisierten Applikators, Optimierung und erste Patientenbehandlungen.** *Rofo*. 2003: 393–400. DOI: 10.1055/s-2003-37830
- 25 Chouillard EK, Gumbs AA, Cherqui D. **Vascular clamping in liver surgery: physiology, indications and techniques.** *Ann Surg Innov Res*. 2010: 2. DOI: 10.1186/1750-1164-4-2
- 26 Ercolani G, Ravaioli M, Grazi GL et al. **Use of vascular clamping in hepatic surgery: lessons learned from 1260 liver resections.** *Arch Surg*. 2008: 380-7; discussion 388. DOI: 10.1001/archsurg.143.4.380
- 27 Lesurtel M, Lehmann K, Rougemont O de et al. **Clamping techniques and protecting strategies in liver surgery.** *HPB*. 2009: 290–295. DOI: 10.1111/j.1477-2574.2009.00066.x
- 28 Vogl TJ, Mack MG, Roggan A et al. **Internally cooled power laser for MR-guided interstitial laser-induced thermotherapy of liver lesions: initial clinical results.** *Radiology*. 1998: 381–385. DOI: 10.1148/radiology.209.2.9807562
- 29 Regier M, Chun F. **Thermal Ablation of Renal Tumors: Indications, Techniques and Results.** *Dtsch Arztebl Int*. 2015: 412–418. DOI: 10.3238/arztebl.2015.0412
-

-
- 30 Stroszczyński C, Gaffke G, Gnauck M et al. **Aktueller Stand und Entwicklungen der Laserablation in der Tumortherapie.** *Radiologe.* 2004: 320–329. DOI: 10.1007/s00117-004-1034-8
- 31 Ahmed M, Solbiati L, Brace CL et al. **Image-guided tumor ablation: standardization of terminology and reporting criteria--a 10-year update.** *Radiology.* 2014: 241–260. DOI: 10.1148/radiol.14132958
- 32 Ichida K. **Significance of the Difference in the Size of Liver Tumors in the Management of Patients with Colorectal Liver Metastases.** *Journal of Molecular and Genetic Medicine.* 2017. DOI: 10.4172/1747-0862.1000254
- 33 Wang X, Wang Z, Wu L. **Combined measurements of tumor number and size helps estimate the outcome of resection of Barcelona clinic liver cancer stage B hepatocellular carcinoma.** *BMC Surg.* 2016: 22. DOI: 10.1186/s12893-016-0135-4
- 34 Partelli S, Mukherjee S, Mawire K et al. **Larger hepatic metastases are more frequent with N0 colorectal tumours and are associated with poor prognosis: implications for surveillance.** *Int J Surg.* 2010: 453–457. DOI: 10.1016/j.ijso.2010.05.013
- 35 Wu G, Wu J, Wang B et al. **Importance of tumor size at diagnosis as a prognostic factor for hepatocellular carcinoma survival: a population-based study.** *Cancer Manag Res.* 2018: 4401–4410. DOI: 10.2147/CMAR.S177663
- 36 An C, Jiang Y, Huang Z et al. **Assessment of Ablative Margin After Microwave Ablation for Hepatocellular Carcinoma Using Deep Learning-Based Deformable Image Registration.** *Front Oncol.* 2020: 573316. DOI: 10.3389/fonc.2020.573316
- 37 Reig M, Forner A, Rimola J et al. **BCLC strategy for prognosis prediction and treatment recommendation: The 2022 update.** *Journal of Hepatology.* 2022: 681–693. DOI: 10.1016/j.jhep.2021.11.018
- 38 Weigel C, Kirsch M, Mensel B et al. **Perkutane laserinduzierte Thermoablation von Lungenmetastasen: Erfahrungen nach 4-jähriger Anwendung.** *Radiologe.* 2004: 700–707. DOI: 10.1007/s00117-004-1083-z

-
- 39 Pruitt R, Gamble A, Black K et al. **Complication avoidance in laser interstitial thermal therapy: lessons learned.** *J Neurosurg.* 2017: 1238–1245. DOI: 10.3171/2016.3.JNS152147
- 40 Namakshenas P, Mojra A. **Optimization of polyethylene glycol-based hydrogel rectal spacer for focal laser ablation of prostate peripheral zone tumor.** *Phys Med.* 2021: 104–113. DOI: 10.1016/j.ejmp.2021.07.034
- 41 Ishikawa T, Kubota T, Horigome R et al. **Radiofrequency ablation during continuous saline infusion can extend ablation margins.** *World J Gastroenterol.* 2013: 1278–1282. DOI: 10.3748/wjg.v19.i8.1278
- 42 Björelund U, Notstam K, Fransson P et al. **Hyaluronic acid spacer in prostate cancer radiotherapy: dosimetric effects, spacer stability and long-term toxicity and PRO in a phase II study.** *Radiat Oncol.* 2023: 1. DOI: 10.1186/s13014-022-02197-x
- 43 Mankertz F, Gemeinhardt O, Felbor U et al. **Spacer-Supported Thermal Ablation to Prevent Carbonisation and Improve Ablation Size: A Proof of Concept Study.** *Biomedicines.* 2023: 575. DOI: 10.3390/biomedicines11020575
- 44 Al-Mohamady AE-SAE-H, Ibrahim SMA, Muhammad MM. **Pulsed dye laser versus long-pulsed Nd:YAG laser in the treatment of hypertrophic scars and keloid: A comparative randomized split-scar trial.** *Journal of cosmetic and laser therapy : official publication of the European Society for Laser Dermatology.* 2016: 208–212. DOI: 10.3109/14764172.2015.1114648
- 45 Joffe SN, Oguro Y. **Advances in Nd-YAG laser surgery.** 1st ed. 1988. New York: Springer-Verlag. 1988.). DOI: 10.1007/978-1-4612-3728-0
- 46 Kim JW, Du Moon G. **Basic Principles of Laser for Prostate Surgery.** *Korean J Androl.* 2011: 101. DOI: 10.5534/kja.2011.29.2.101
- 47 Fisher JC. **A Brief History of the Nd:YAG Laser.** *Advances in Nd-YAG laser surgery.* 1st ed. 1988. New York: Springer-Verlag. 1988: 7–9. DOI: 10.1007/978-1-4612-3728-0_2

-
- 48 Landro M de, Espíritu García-Molina I, Barberio M et al. **Hyperspectral Imagery for Assessing Laser-Induced Thermal State Change in Liver.** *Sensors (Basel)*. 2021. DOI: 10.3390/s21020643
- 49 Jacques SL. **Laser-tissue interactions. Photochemical, photothermal, and photomechanical.** *Surg Clin North Am*. 1992: 531–558. DOI: 10.1016/s0039-6109(16)45731-2
- 50 Carroll L, Humphreys TR. **LASER-tissue interactions.** *Clin Dermatol*. 2006: 2–7. DOI: 10.1016/j.clindermatol.2005.10.019
- 51 Jawad MM, Abdul Qade ST, Zaidan AA et al. **An Overview of Laser Principle, Laser-Tissue Interaction Mechanisms and Laser Safety Precautions for Medical Laser Users.** *International J. of Pharmacology*. 2011: 149–160. DOI: 10.3923/ijp.2011.149.160
- 52 Schena E, Saccomandi P, Fong Y. **Laser Ablation for Cancer: Past, Present and Future.** *J Funct Biomater*. 2017. DOI: 10.3390/jfb8020019
- 53 Stafford RJ, Fuentes D, Elliott AA et al. **Laser-induced thermal therapy for tumor ablation.** *Crit Rev Biomed Eng*. 2010: 79–100. DOI: 10.1615/critrevbiomedeng.v38.i1.70
- 54 Dabbs EB, Riley MI, Davies CE et al. **Pattern of thermal damage and tissue carbonisation from endovenous radiofrequency ablation catheter - Using an in vitro porcine liver model.** *Phlebology*. 2021: 489–495. DOI: 10.1177/0268355520975539
- 55 Weigel C, Rosenberg C, Langner S et al. **Laser ablation of lung metastases: results according to diameter and location.** *European radiology*. 2006: 1769–1778. DOI: 10.1007/s00330-006-0171-z
- 56 Andres M. **Improving thermal ablation of liver tumours:: Modeling and parameter identification of laser-induced interstitial thermotherapy** [*Doctoral Thesis*]. Kaiserslautern: Technische Universität, 2021. DOI: 10.26204/KLUEDO/6322
- 57 Vorobyev AY, Guo C. **Reflection of femtosecond laser light in multipulse ablation of metals.** *Journal of Applied Physics*. 2011: 43102. DOI: 10.1063/1.3620898

-
- 58 Welch AJ, Motamedi M, Rastegar S et al. **Laser thermal ablation.** *Photochem Photobiol.* 1991: 815–823. DOI: 10.1111/j.1751-1097.1991.tb09896.x
- 59 Ashraf O, Patel NV, Hanft S et al. **Laser-Induced Thermal Therapy in Neuro-Oncology: A Review.** *World Neurosurg.* 2018: 166–177. DOI: 10.1016/j.wneu.2018.01.123
- 60 Chu KF, Dupuy DE. **Thermal ablation of tumours: biological mechanisms and advances in therapy.** *Nat Rev Cancer.* 2014: 199–208. DOI: 10.1038/nrc3672
- 61 Laimer G, Jaschke N, Schullian P et al. **Volumetric assessment of the periablational safety margin after thermal ablation of colorectal liver metastases.** *European radiology.* 2021: 6489–6499. DOI: 10.1007/s00330-020-07579-x
- 62 Kühn JP, Puls R, Wallaschowski H et al. **Charakteristik von Koagulationsnekrosen nach laserinduzierter Thermotherapie in der kontrastmittelverstärkten Magnetresonanztomografie und deren Einfluss auf den Therapieerfolg.** *Rofo.* 2008: 816–820. DOI: 10.1055/s-2008-1027478
- 63 Fahrenholtz SJ, Moon TY, Franco M et al. **A model evaluation study for treatment planning of laser-induced thermal therapy.** *Int J Hyperthermia.* 2015: 705–714. DOI: 10.3109/02656736.2015.1055831
- 64 Lewandowski MA, Hinz MW. **A simple approach to industrial laser safety.** *Health Phys.* 2005: S24-30. DOI: 10.1097/01.hp.0000147793.62405.4c
- 65 Bartov E, Rock T, Treister G et al. **Total internal reflection of laser light in eyes filled with silicone oil.** *Ophthalmic Surg Lasers; 30 (1) 1999: 17–23*
- 66 Yan X-L, Dong S-Y, Xu B-S et al. **Progress and Challenges of Ultrasonic Testing for Stress in Remanufacturing Laser Cladding Coating.** *Materials (Basel).* 2018. DOI: 10.3390/ma11020293
- 67 Dellmann H-D. **Dellmans textbook of veterinary histology.** 6th ed. Ames, IO: Blackwell. Dellmann H-D. 2006. 405p.
- 68 Viard R, Emptaz A, Piron B et al. **Determination of the lesion size in Laser-induced Interstitial Thermal Therapy (LITT) using a low-field MRI.** *Annu Int Conf IEEE Eng Med Biol Soc.* 2007: 214–217. DOI: 10.1109/IEMBS.2007.4352261

-
- 69 Carpentier A, McNichols RJ, Stafford RJ et al. **Laser thermal therapy: real-time MRI-guided and computer-controlled procedures for metastatic brain tumors.** *Lasers in surgery and medicine.* 2011: 943–950. DOI: 10.1002/lsm.21138
- 70 Jahn A. **Gadoxetic acid for contrast-enhanced MR-guided laser ablation of liver malignancies with Thermometry.** University Clinic Greifswald, 2012
- 71 Minami Y, Kudo M. **Image Guidance in Ablation for Hepatocellular Carcinoma: Contrast-Enhanced Ultrasound and Fusion Imaging.** *Front Oncol.* 2021: 593636. DOI: 10.3389/fonc.2021.593636
- 72 Goldberg SN, Gazelle GS, Mueller PR. **Thermal ablation therapy for focal malignancy: a unified approach to underlying principles, techniques, and diagnostic imaging guidance.** *AJR. American journal of roentgenology.* 2000: 323–331. DOI: 10.2214/ajr.174.2.1740323
- 73 Peters BS, Dornaika R, Hosten N et al. **Regression of cardiac hypertrophy in cyp1a1ren-2 transgenic rats.** *J Magn Reson Imaging.* 2012: 373–378. DOI: 10.1002/jmri.23661
- 74 Hemmerich W. **Entscheidungshilfe für statistische Verfahren.** Wiesbaden (2023). Im Internet: statistikguru.de/test-entscheidungshilfe/dtCp.html; Stand: 17.02.2023, 16:35
- 75 Collins LM. **Research Design and Methods.** *Encyclopedia of Gerontology:* 433–442. DOI: 10.1016/B0-12-370870-2/00162-1
- 76 Koo TK, Li MY. **A Guideline of Selecting and Reporting Intraclass Correlation Coefficients for Reliability Research.** *J Chiropr Med.* 2016: 155–163. DOI: 10.1016/j.jcm.2016.02.012
- 77 Hui TC, Kwan J, Pua U. **Advanced Techniques in the Percutaneous Ablation of Liver Tumours.** *Diagnostics (Basel).* 2021. DOI: 10.3390/diagnostics11040585
- 78 Kim C. **Understanding the nuances of microwave ablation for more accurate post-treatment assessment.** *Future Oncol.* 2018: 1755–1764. DOI: 10.2217/fon-2017-0736

-
- 79 Payne M, Bossmann SH, Basel MT. **Direct treatment versus indirect: Thermo-ablative and mild hyperthermia effects.** *Wiley Interdiscip Rev Nanomed Nanobiotechnol.* 2020: e1638. DOI: 10.1002/wnan.1638
- 80 Amabile C, Farina L, Lopresto V et al. **Tissue shrinkage in microwave ablation of liver: an ex vivo predictive model.** *Int J Hyperthermia.* 2017: 101–109. DOI: 10.1080/02656736.2016.1208292
- 81 Atsumi H, Matsumae M, Kaneda M et al. **Novel laser system and laser irradiation method reduced the risk of carbonization during laser interstitial thermotherapy: assessed by MR temperature measurement.** *Lasers Surg. Med.* 2001: 108–117. DOI: 10.1002/lsm.1096
- 82 Wang Y, Sun Y, Feng L et al. **Internally cooled antenna for microwave ablation: results in ex vivo and in vivo porcine livers.** *European Journal of Radiology.* 2008: 357–361. DOI: 10.1016/j.ejrad.2007.07.015
- 83 Hosten N. **MRI-Guided Laser Ablation In The Liver.** *Interventional Magnetic Resonance Imaging:* 289–302
- 84 Shi X, Pan H, Ge H et al. **Subsequent cooling-circulation after radiofrequency and microwave ablation avoids secondary indirect damage induced by residual thermal energy.** *Diagn Interv Radiol.* 2019: 291–297. DOI: 10.5152/dir.2019.17455
- 85 Rogers W. **What are the typical temperature ratings on lab glassware? Im Internet:** www.aceglass.com/dpro/kb_article.php?ref=4347-TFBN-1216; Stand: 31.08.2022, 09:52
- 86 Eppendorf SE. **epT.I.P.S.® Standard - Instructions for Use.** Hamburg, Germany. Im Internet: www.eppendorf.com/de-de/eShop-Produkte/Spitzen-Reaktionsgef%C3%A4%C3%9Ffe-und-Platten/Pipettenspitzen/epTIPS-p-0030000870; Stand: 31.08.2022, 10:46
- 87 Madhan KE. **Comparative histology of human and cow, goat and sheep liver.** *Journal of Surgical Academia;* 4 (1) 2014: 10–13
- 88 Estermann S-J, Förster-Streffleur S, Hirtler L et al. **Comparison of Thiel preserved, fresh human, and animal liver tissue in terms of mechanical properties.** *Ann Anat.* 2021: 151717. DOI: 10.1016/j.aanat.2021.151717
-

-
- 89 Fang Z, Zhang B, Zhang W. **Current Solutions for the Heat-Sink Effect of Blood Vessels with Radiofrequency Ablation: A Review and Future Work.** *Advanced computational methods in life system modeling and simulation*. Singapore: Springer. 2017: 113–122. DOI: 10.1007/978-981-10-6370-1_12
- 90 Mensel B, Weigel C, Heidecke C-D et al. **Laserinduzierte Thermotherapie (LITT) von Lebertumoren in zentraler Lokalisation: Ergebnisse und Komplikationen.** *Rofo*. 2005: 1267–1275. DOI: 10.1055/s-2005-858329
- 91 Wacker FK, Reither K, Ritz JP et al. **MR-guided interstitial laser-induced thermotherapy of hepatic metastasis combined with arterial blood flow reduction: Technique and first clinical results in an open MR system.** *J. Magn. Reson. Imaging*. 2001: 31–36. DOI: 10.1002/1522-2586(200101)13:1<31::AID-JMRI1005>3.0.CO;2-I
- 92 Hosten N. **Suppressing portal vein perfusion by a percutaneously introduced balloon.** [Unpublished study provided to the author]. Greifswald, 2022
- 93 Roesler M. **Experimentelle Evaluation der Laser-induzierten Thermotherapie (LITT) an ex-vivo Rinderleber unter Verwendung zweier Kühlmedien.** Berlin: University Clinic Charité, 2005
- 94 El Sawaf Y, Anetsberger S, Luzzi S et al. **Three-Dimensional Volumetric Assessment of Resected Gliomas Assisted by Horos Imaging Software: Video Case Series of Postoperative Tumor Analyses.** *Cureus*. 2021: e13571. DOI: 10.7759/cureus.13571
- 95 Vogl TJ, Zangos S, Balzer JO et al. **Transarterielle Chemoembolisation (TACE) des hepatozellulären Karzinoms: Technik, Indikationsstellung und Ergebnisse.** *Rofo*. 2007: 1113–1126. DOI: 10.1055/s-2007-963285
- 96 Butt OH, Zhou AY, Huang J et al. **A phase II study of laser interstitial thermal therapy combined with doxorubicin in patients with recurrent glioblastoma.** *Neurooncol Adv*. 2021: vdab164. DOI: 10.1093/noajnl/vdab164
- 97 Pacella CM, Bizzarri G, Cecconi P et al. **Hepatocellular carcinoma: long-term results of combined treatment with laser thermal ablation and transcatheter arterial chemoembolization.** *Radiology*. 2001: 669–678. DOI: 10.1148/radiology.219.3.r01ma02669
-

-
- 98 Chen J, Burns FP, Moffitt MG et al. **Thermally Crosslinked Functionalized Polydicyclopentadiene with a High Tg and Tunable Surface Energy.** *ACS Omega.* 2016: 532–540. DOI: 10.1021/acsomega.6b00193
- 99 Gross BC, Erkal JL, Lockwood SY et al. **Evaluation of 3D printing and its potential impact on biotechnology and the chemical sciences.** *Anal Chem.* 2014: 3240–3253. DOI: 10.1021/ac403397r
- 100 Bakhshaeekia A, Yarmohammadi H, Abbasi HR. **Polytetrafluoroethylene (Gore-Tex) tube used as a support conduit in open gastrostomy: report of a new technique.** *Int J Surg.* 2010: 35–38. DOI: 10.1016/j.ijso.2009.09.015
- 101 Jeyanathan J, Webster BB, Hawksley OJ et al. **A comparison of performance between Teflon and polyurethane safety cannulae at extremes of operating temperatures.** *J R Army Med Corps.* 2012: 120–122. DOI: 10.1136/jramc-158-02-10
- 102 Rosenberg C, Hoffmann COM, Mensel B et al. **Laserablation. Brauchen wir sie noch?** *Radiologe.* 2012: 15–21. DOI: 10.1007/s00117-011-2207-x
- 103 Vogl TJ, Farshid P, Naguib NNN et al. **Thermal ablation of liver metastases from colorectal cancer: radiofrequency, microwave and laser ablation therapies.** *Radiol Med.* 2014: 451–461. DOI: 10.1007/s11547-014-0415-y
- 104 Izzo F. **Other thermal ablation techniques: microwave and interstitial laser ablation of liver tumors.** *Ann Surg Oncol.* 2003: 491–497. DOI: 10.1245/aso.2003.07.016
- 105 Poulou LS, Botsa E, Thanou I et al. **Percutaneous microwave ablation vs radiofrequency ablation in the treatment of hepatocellular carcinoma.** *World J Hepatol.* 2015: 1054–1063. DOI: 10.4254/wjh.v7.i8.1054
- 106 Ozen M, Raissi D. **Current perspectives on microwave ablation of liver lesions in difficult locations.** *J Clin Imaging Sci.* 2022: 61. DOI: 10.25259/JCIS_126_2022
- 107 Vogl TJ, Nour-Eldin N-EA, Hammerstingl RM et al. **Mikrowellenablation (MWA): Grundlagen, Technik und Ergebnisse in primären und sekundären Lebertumoren – Übersichtsarbeit.** *Rofo.* 2017: 1055–1066. DOI: 10.1055/s-0043-117410

108 Takahashi H, Berber E. **Role of thermal ablation in the management of colorectal liver metastasis.** *Hepatobiliary Surg Nutr.* 2020: 49–58. DOI: 10.21037/hbsn.2019.06.08



Article

Spacer-Supported Thermal Ablation to Prevent Carbonisation and Improve Ablation Size: A Proof of Concept Study

Fiona Mankertz ^{1,*}, Ole Gemeinhardt ², Ute Felbor ³, Stefan Hadlich ¹ and Norbert Hosten ¹¹ Institute for Diagnostic Radiology and Neuroradiology, University Medicine Greifswald, 17475 Greifswald, Germany² Department of Radiology, Charité—Universitätsmedizin Berlin, 10117 Berlin, Germany³ Institute for Human Genetics, University Medicine Greifswald, 17475 Greifswald, Germany

* Correspondence: fiona.mankertz@uni-greifswald.de

Abstract: Thermal ablation offers a minimally invasive alternative in the treatment of hepatic tumours. Several types of ablation are utilised with different methods and indications. However, to this day, ablation size remains limited due to the formation of a central non-conductive boundary layer. In thermal ablation, this boundary layer is formed by carbonisation. Our goal was to prevent or delay carbonisation, and subsequently increase ablation size. We used bovine liver to compare ablation diameter and volume, created by a stand-alone laser applicator, with those created when utilising a spacer between laser applicator and hepatic tissue. Two spacer variants were developed: one with a closed circulation of cooling fluid and one with an open circulation into hepatic tissue. We found that the presence of a spacer significantly increased ablation volume up to 75.3 cm³, an increase of a factor of 3.19 (closed spacer) and 3.02 (open spacer) when compared to the stand-alone applicator. Statistical significance between spacer variants was also present, with the closed spacer producing a significantly larger ablation volume ($p < 0.001$, $M_{Diff} = 3.053$, 95% CI[1.612, 4.493]) and diameter ($p < 0.001$, $M_{Diff} = 4.467$, 95% CI[2.648, 6.285]) than the open spacer. We conclude that the presence of a spacer has the potential to increase ablation size.

Keywords: thermal ablation; laser ablation; experimental radiology; ablation zone; Nd:YAG

Citation: Mankertz, F.; Gemeinhardt, O.; Felbor, U.; Hadlich, S.; Hosten, N. Spacer-Supported Thermal Ablation to Prevent Carbonisation and Improve Ablation Size: A Proof of Concept Study. *Biomedicines* **2023**, *11*, 575. <https://doi.org/10.3390/biomedicines11020575>

Academic Editor: Ryszard Smolarczyk

Received: 23 January 2023

Revised: 13 February 2023

Accepted: 13 February 2023

Published: 16 February 2023



Copyright: © 2023 by the authors. Licensee MDPI, Basel, Switzerland. This article is an open access article distributed under the terms and conditions of the Creative Commons Attribution (CC BY) license (<https://creativecommons.org/licenses/by/4.0/>).

1. Introduction

The development of minimally invasive procedures has conferred the possibility of eliminating primary and secondary hepatic lesions. Over the last three decades, minimally invasive ablation has been established as a safe and effective alternative to conventional surgery. Tumour ablation is categorised in non-energy based ablation such as trans-arterial chemoembolisation (TACE) and energy-based ablation, the latter of which can be further separated into thermal and non-thermal ablation. Today, the most frequently used procedure is thermal ablation, with several well-documented and clinically studied methods such as radiofrequency ablation (RFA), microwave ablation (MWA) and laser ablation (LA). Whilst those methods differ in regard to their physical principles, they all share the same goal: the complete thermal ablation of tumorous tissue with an adequate margin of non-tumorous tissue. However, the maximum achievable ablation size has proven to be the greatest limitation for all those methods [1].

Ablation size (both in volume and diameter) is limited due to the transformation of viable energy-conducting tissue into a boundary layer which does not conduct energy efficiently. In thermal ablation, this process is known as carbonisation. Carbonisation occurs when tissue temperatures rise above 100 °C. As biological tissue is sensitive to external stress, a sudden increase in temperature leads to protein denaturation, the dissolution of hydrogen bonds and DNA polymerase inhibition [2]. At temperatures of over 45 °C, irreversible cell damage occurs. This process is sped up exponentially with further increases in temperature; it is the principle on which the thermal ablation of tumorous tissues relies

thermal ablation, no histopathological sample is obtained to confirm the full ablation of tumorous tissue. Subsequently, they examined the relationship between peri-ablative invasive temperature measurements and post-ablative histopathological examination. They found that tissue confirmed as non-viable in 2,3,5-triphenyltetrazolium chloride viability staining could be macroscopically distinguished from viable tissue by its different colouring, as well as changes in tissue density. This macroscopically defined non-viable tissue also matched the necrotic areas found on H&E staining. In a 2011 study, Schneider et al. additionally found that non-viable pulmonal tissue following radiofrequency ablation could not be differentiated from viable tissue using standard H&E staining alone [17,18]. As such, we chose to forego histological staining due to the clear evidence of correlation with macroscopic findings.

We conceptualised and produced a spacer in a miniseries for the purpose of conducting several experiments. The spacer augmented the distance between the laser's optical fibre and tissue through the generation of a fluid-filled space. Two main variants of the spacer were created: one with a closed tip where diffusion fluid served as a cooling agent and circulated internally, as well as one with an open tip where the diffusion fluid was diffused into the surrounding hepatic tissue (see Figure 1).

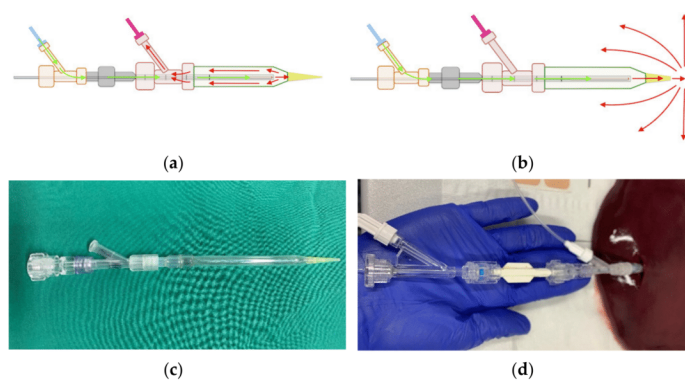


Figure 1. Diffusion circulation in the (a) closed spacer circuit and (b) open spacer circuit. Cooling fluid circulates through the spacer at a temperature of 20 °C and (a) drains into an external calorimeter or (b) diffuses into external tissue. In (c) is shown the real closed spacer prototype, as well as (d) the experimental setup using the closed spacer.

Figure 1 shows the spacer with closed (a) and open (b) diffusion circulation. Isotone sodium chloride solution (0.9%) was used as a cooling agent. In a preceding experimental study, we found that there was no significant difference between the usage of sodium chloride and aqua destillata. Aqua destillata has the added disadvantage of its hypo-osmolar properties, which is less suitable for continuous infusion into the human body than 0.9% sodium chloride [15]. Additionally, Ishikawa et al. reported in 2013 that radiofrequency ablation produced significantly larger ablation zones when combined with the continuous infusion of saline solution. They also noted that when using a hypotone 50% glucose solution, ablation zones were diminished even in comparison to not infusing any fluid [14]. As such, we chose sodium chloride solution for its well-established compatibility with the human body and its efficacy in ablation therapy. Both spacers were filled with the cooling agent before tissue insertion, and fluid was diffused through means of a peristaltic pump at a set rate of 60 mL/h. The spacers were constructed from commercially available components: a glass pipette (B. Braun Melsungen, Melsungen, Germany) with a diameter

of 4 mm, a distal 200 μ L polypropylene pipette tip, as well as a proximal Y-connector (Figure 1c).

To ensure realistic ex vivo simulation, bovine livers ($n = 15$) were chosen due to their similarities to human liver in regard to capsule density and tissue structure. The livers were acquired from an abattoir (LandWert Hof, Stahlbrode, Sundhagen, Germany) <1 h post-slaughter and transported in a heat-resistant styrofoam container at room temperature. Pre-ablation, all livers were examined by a public health veterinarian. Any remains of adjunct structures and omental fat were removed to ensure tissue homogeneity. Large vessels such as portal and caval veins, hepatic arteries, or the biliary duct were longitudinally incised to prevent fluid diffusion into air-filled vessels. Any hepatic tissue measured to be <100 mm in diameter was also removed. The stand-alone applicator or spacer-supported applicator were first filled with commercial saline solution and then inserted into hepatic tissue up to the proximal Y-connector (Figure 1d).

The process of laser ablation with a commercially available applicator system (RoweMed, Parchim, Germany) has been documented in several studies and was utilised according to standard practice [9]. The term “stand-alone applicator system” refers to the conglomerate of optical fibre enveloped by a diffusion catheter and a proximal Y-connector. For the purpose of our study, we used a Medilas Fibertom 5100 laser with a Nd:YAG 1064 nm wavelength (Dornier Medtech Europe GmbH, Munich, Germany).

In order to determine the maximal wattage we could use without the occurrence of carbonisation, the laser’s power was increased from 15 W to 35 W in 5 W increments at a set time interval of 10 min until carbonisation was recorded. Subsequently, the lasing time interval was increased from 5 min to 30 min in 5 min increments at a set wattage of 25 W until carbonisation was recorded.

For the stand-alone applicator system, the maximum combination of wattage and time interval was 25 W and 10 min. For the spacer-supported applicator systems, the maximum combination was 25 W and 25 min. To facilitate comparison between not only the stand-alone applicator system and the spacers, but also between the spacers, we conducted an *interspacial* trial with all three experimental designs at 25 W and 10 min, as well as an *intraspacial* trial with both spacer variants at 25 W and 25 min.

At the end of each LA procedure, the tissue was sliced along the antenna tract, revealing a cross section of the ablation zone. Ablation zones are defined by their cell viability, as correlated by vitality staining and standard H&E staining in external studies [17,18]. The central zone (black overlay in Figure 2a) is the carbonised boundary layer of charred, non-conductive tissue. The proximal zone of ablation (green overlay in Figure 2a,b) is comprised of fully ablated, non-viable tissue. The distal zone (white overlay in Figure 2a,b) has both viable and non-viable tissue. Gemeinhardt et al. also separated the zone of partial ablation into a “red zone 1”, in which vital and non-vital cells comprise a similar percentage, as well as a “red zone 2” in which cells are mostly vital [19]. All three ablation zones were measured, and their longitudinal, perpendicular and vertical diameter was recorded.

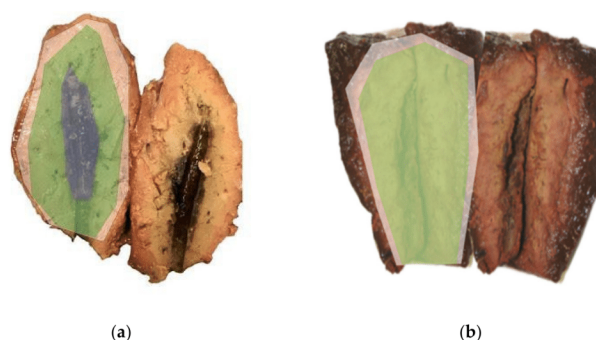


Figure 2. Cross section of the ablation zones in (a) the stand-alone applicator (25 W; 10 min) and (b) the spacer-supported applicator (25 W; 25 min). Black overlay: carbonisation zone. Green overlay: non-viable tissue. White overlay: total ablation zone (“red zone”).

2.2. Volumetry

As MRI imaging is the standard method for periprocedural thermometry and postprocedural monitoring for laser ablation, post-ablation scans were obtained on a 7T. ClinScan 70/30 Biospec MRI USR (Bruker BioSpin GmbH, Bruker Scientific Instruments, Ettlingen, Germany). T1 weighted FL2D imaging was performed due to its superior differentiation of signal loss caused by tissue coagulation. Coagulation presented as hyperintense in comparison to liver tissue. Volumetry was conducted through a standard DICOM viewer. Sagittal and horizontal sequences were analysed, and closed-polygon area was calculated. Following a conclusive area selection, tissue coagulation volume was calculated through ROI volumetry (V_{MRI}).

Additionally, tissue coagulation volume was manually measured through displacement volumetry (V_D). Displacement volumetry relies on Archimedes’ principle that the volume of a buoyant submerged object is equal to the weight of the fluid displaced by the object ($m = V$). Post-MRI, the ablated tissue was debrided into an ellipsoid shape, and the mass of the water displaced by the ellipsoid tissue was weighed ($1\text{ g} = 1\text{ cm}^3$). Post-MRI DICOM volumetry was compared with displacement volumetry to prevent type I errors.

As seen in Table 1, we found that there was no significant difference between the two methods of volumetric analysis, as the level of statistical significance was consistently >0.05 . We thus chose to proceed to measure tissue coagulation volume through displacement volumetry. MRI volumetry may be utilised in later studies in the knowledge that it accurately represents non-viable tissue boundaries.

Table 1. Calculated p -value between V_{MRI} and V_D .

Comparisons	Two-Tailed p Value between V_{MRI} and V_D	Mean Difference	95% Confidence Interval of Difference
S_N (25 W 10 min)	0.9228	−0.0507	−1.1126 to 1.0112
S_C (25 W 10 min)	0.1216	0.5507	−0.1558 to 1.2572
S_O (25 W 10 min)	0.1302	0.6327	−0.1985 to 1.4638
S_C (25 W 25 min)	0.9400	0.0687	−1.7832 to 1.9206
S_O (25 W 25 min)	0.8328	−0.1040	−1.1035 to 0.8955

V_{MRI} : ROI volumetry; V_D : displacement volumetry; S_N : stand-alone applicator; S_C : closed spacer-supported applicator; S_O : open spacer-supported applicator.

\emptyset_P : $F(2,42) = 148.735, p < 0.001$, partial $\eta^2 = 0.876$

V_{MRI} : $F(2,42) = 82.057, p < 0.001$, partial $\eta^2 = 0.796$

V_D : $F(2,42) = 99.085, p < 0.001$, partial $\eta^2 = 0.825$

Finally, a Games-Howell post hoc analysis was performed to ascertain the quality of statistical significance. Pairwise differences in ablation volume and perpendicular diameter were also found to be statistically significant.

4. Discussion

Over the past two decades, thermal ablation and its different energy sources have been established as a valid treatment option of hepatic lesions, specifically hepatocellular carcinoma and metastases. While different types of thermal ablation such as RFA, MWA and LA differ by practicability, cost efficiency, as well as absolute and relative contraindications, a main limitation of each method remains its achievable tissue coagulation size. Small lesions up to 30 mm can be fully ablated when including a safe margin [21], while medium-sized lesions with a diameter of 30–50 mm are unable to be fully ablated with a single applicator in only one application [1]. The full ablation of tumours between 30–50 mm is only possible through multiple applicators or several rounds of applications and differing applicator positioning, as well as the addition of surgical and interventional techniques such as vascular clamping [2] and TACE [1]. Vascular clamping of the total, partial or selective hepatic flow is a valid method. However, it is technically demanding, shows association with intestinal congestion and requires an intermittent or continuous period of organ ischemia [10,11].

The size limitation in thermal ablation is caused by overheating near the thermal applicator, which at a certain point transforms viable heat-conducting tissue into a non-conductive boundary layer. This boundary layer acts as an insulating “shell”, which limits further energy transmission into peripheral tissue. In RFA, abrupt changes in tissue impedance have been reported to create “heat spots” around the probes [22]. In MWA and LA, the formation of a boundary layer has been described as carbonisation around the applicators [23]. Preventing carbonisation has been key in increasing ablation size, as several developments in recent years show: For MWA in recent years, an internal cooling jacket has been developed [24]. RFA and LA have been improved through the standardised development of cooling diffusers [25,26]. These improvements share similar aims and methods; their goal is the increase in energy diffusion through the targeted tissue by decreasing the temperature immediately adjacent to the heat source.

A second approach to maximise ablation size is the usage of higher wattage and longer ablation times. As the output and transmission of energy is directly linear to power input and time interval $E = P \cdot t$, conducting an ablation protocol with higher power would result in higher ablation volume and diameter. However, when power is set too high, central tissue temperatures rise exponentially and carbonisation occurs much faster [27]. In our preliminary studies, to determine optimal wattage, we noted that any power above 25 W would lead to almost instantaneous abortion of the ablation process. Conversely, low power, such as 5 W or 10 W, would allow longer ablation time intervals, but ultimately resulted in a smaller ablation size. We thus selected a power input of 25 W.

A technically comparatively simple and cost-effective approach to prevent these thermal changes of tissue is the usage of a spacer. It creates an artificial, fluid-filled space between the applicator and the targeted, viable tissue. The concept behind the spacer’s efficacy has not been fully explained up to this point; however, there are two hypotheses.

- I. The hypothesis of **optical gain**: photons travel through the spacer’s fluid medium before entering hepatic tissue. As the absorption coefficient in the liquid medium is low, the laser’s stimulated emission is not absorbed until it enters hepatic tissue. In hepatic tissue, the absorption coefficient rises sharply, and photothermal interactions take place after absorption [28].
- II. The hypothesis of **heat diffusion**: similar to how the physiological heat sink effect limits ablation size close to larger vessels [29], the constant diffusion of fluid

23. Amabile, C.; Farina, L.; Lopresto, V.; Pinto, R.; Cassarino, S.; Tosoratti, N.; Goldberg, S.N.; Cavagnaro, M. Tissue shrinkage in microwave ablation of liver: An ex vivo predictive model. *Int. J. Hypertherm.* **2017**, *33*, 101–109. [[CrossRef](#)]
24. Wang, Y.; Sun, Y.; Feng, L.; Gao, Y.; Ni, X.; Liang, P. Internally cooled antenna for microwave ablation: Results in ex vivo and in vivo porcine livers. *Eur. J. Radiol.* **2008**, *67*, 357–361. [[CrossRef](#)]
25. Shi, X.; Pan, H.; Ge, H.; Li, L.; Xu, Y.; Wang, C.; Xie, H.; Liu, X.; Zhou, W.; Wang, S. Subsequent cooling-circulation after radiofrequency and microwave ablation avoids secondary indirect damage induced by residual thermal energy. *Diagn. Interv. Radiol.* **2019**, *25*, 291–297. [[CrossRef](#)] [[PubMed](#)]
26. Vogl, T.J.; Mack, M.G.; Roggan, A.; Straub, R.; Eichler, K.C.; Muller, P.K.; Knappe, V.; Félix, R. Internally cooled power laser for MR-guided interstitial laser-induced thermotherapy of liver lesions: Initial clinical results. *Radiology* **1998**, *209*, 381–385. [[CrossRef](#)] [[PubMed](#)]
27. Gough-Palmer, A.L.; Gedroyc, W.M. Laser ablation of hepatocellular carcinoma—A review. *World J. Gastroenterol.* **2008**, *14*, 7170–7174. [[CrossRef](#)]
28. Germer, C.T.; Roggan, A.; Ritz, J.P.; Isbert, C.; Albrecht, D.; Müller, G.; Buhr, H.J. Optical properties of native and coagulated human liver tissue and liver metastases in the near infrared range. *Lasers Surg. Med.* **1998**, *23*, 194–203. [[CrossRef](#)]
29. Kim, C. Understanding the nuances of microwave ablation for more accurate post-treatment assessment. *Future Oncol.* **2018**, *14*, 1755–1764. [[CrossRef](#)]
30. Laimer, G.; Jaschke, N.; Schullian, P.; Putzer, D.; Eberle, G.; Solbiati, M.; Solbiati, L.; Goldberg, S.N.; Bale, R. Volumetric assessment of the periablational safety margin after thermal ablation of colorectal liver metastases. *Eur. Radiol.* **2021**, *31*, 6489–6499, Erratum in *Eur. Radiol.* **2021**. [[CrossRef](#)] [[PubMed](#)]
31. Pacella, C.M.; Bizzarri, G.; Magnolfi, F.; Cecconi, P.; Caspani, B.; Anelli, V.; Bianchini, A.; Valle, D.; Pacella, S.; Manenti, G.; et al. Laser thermal ablation in the treatment of small hepatocellular carcinoma: Results in 74 patients. *Radiology* **2001**, *221*, 712–720. [[CrossRef](#)]
32. Pacella, C.M.; Bizzarri, G.; Cecconi, P.; Caspani, B.; Magnolfi, F.; Bianchini, A.; Anelli, V.; Pacella, S.; Rossi, Z. Hepatocellular carcinoma: Long-term results of combined treatment with laser thermal ablation and transcatheter arterial chemoembolization. *Radiology* **2001**, *219*, 669–678. [[CrossRef](#)]
33. Hui, T.C.; Kwan, J.; Pua, U. Advanced Techniques in the Percutaneous Ablation of Liver Tumours. *Diagnostics* **2021**, *11*, 585. [[CrossRef](#)] [[PubMed](#)]
34. Brieger, J.; Pereira, P.L.; Trübenbach, J.; Schenk, M.; Kröber, S.-M.; Schmidt, D.; Aubé, C.; Claussen, C.D.; Schick, F. In vivo efficiency of four commercial monopolar radiofrequency ablation systems: A comparative experimental study in pig liver. *Investig. Radiol.* **2003**, *38*, 609–616. [[CrossRef](#)]
35. Poch, F.G.M.; Neizert, C.A.; Gemeinhardt, O.; Geyer, B.; Eminger, K.; Rieder, C.; Niehues, S.M.; Vahldiek, J.; Thieme, S.F.; Lehmann, K.S. Intermittent Pringle maneuver may be beneficial for radiofrequency ablations in situations with tumor-vessel proximity. *Innov. Surg. Sci.* **2018**, *3*, 245–251. [[CrossRef](#)] [[PubMed](#)]
36. Vogl, T.J.; Naguib, N.N.N.; Eichler, K.; Lehnert, T.; Ackermann, H.; Mack, M.G. Volumetric evaluation of liver metastases after thermal ablation: Long-term results following MR-guided laser-induced thermotherapy. *Radiology* **2008**, *249*, 865–871. [[CrossRef](#)] [[PubMed](#)]
37. Poulou, L.S.; Botsa, E.; Thanou, I.; Ziakas, P.D.; Thanos, L. Percutaneous microwave ablation vs radiofrequency ablation in the treatment of hepatocellular carcinoma. *World J. Hepatol.* **2015**, *7*, 1054–1063. [[CrossRef](#)] [[PubMed](#)]
38. Ozen, M.; Raissi, D. Current perspectives on microwave ablation of liver lesions in difficult locations. *J. Clin. Imaging Sci.* **2022**, *12*, 61. [[CrossRef](#)] [[PubMed](#)]
39. Singh, S.; Siriwardana, P.N.; Johnston, E.W.; Watkins, J.; Bandula, S.; Illing, R.; Davidson, B.R. Perivascular extension of microwave ablation zone: Demonstrated using an ex vivo porcine perfusion liver model. *Int. J. Hypertherm.* **2018**, *34*, 1114–1120. [[CrossRef](#)]

Disclaimer/Publisher's Note: The statements, opinions and data contained in all publications are solely those of the individual author(s) and contributor(s) and not of MDPI and/or the editor(s). MDPI and/or the editor(s) disclaim responsibility for any injury to people or property resulting from any ideas, methods, instructions or products referred to in the content.